

**Electrocoagulation as Pretreatment for Fouling Reduction in Forward Osmosis  
Treatment of Shale Gas Produced Water**

Oluchi Okoro

A Thesis  
In The Department of  
Building, Civil and Environmental Engineering

Presented in partial fulfillment of the requirement  
For the Degree of Master of Applied Science (Civil Engineering) at  
Concordia University  
Montreal, Quebec, Canada.  
August 2017

© Oluchi Okoro, 2017

**CONCORDIA UNIVERSITY**

School of Graduate Studies

This is to certify that the thesis prepared

By: Oluchi Okoro

Entitled: Electrocoagulation as Pretreatment for Fouling Reduction in Forward Osmosis Treatment of Shale Gas Produced Water

and submitted in partial fulfillment of the requirements for the degree of

**Master of Applied Science (Civil Engineering)**

complies with the regulations of the University and meets the accepted standards with respect to originality and quality.

Signed by the final Examining Committee:

\_\_\_\_\_ Chair

Dr. Zhi Chen

\_\_\_\_\_ Examiner

Dr. M. Zahangir Kabir

\_\_\_\_\_ Examiner

Dr. Amruthur S. Ramamurthy

\_\_\_\_\_ Supervisor

Dr. Saifur Rahaman

Approved by,

\_\_\_\_\_ Graduate Program Director

Dr. Fariborz Haghighat

\_\_\_\_\_ Dean of Faculty

Dr. Amir Asif

Date: \_\_\_\_\_ 2017

## Abstract

### **Electrocoagulation as a Pretreatment for Fouling Reduction in Forward Osmosis Treatment of Shale Gas Produced Water (SGPW)**

Oluchi Okoro

In this study, the potential of electrocoagulation (EC) as a suitable pretreatment option for shale gas produced water (SGPW) prior to FO was investigated. Specifically, the removal of turbidity, chemical oxygen demand (COD), and three inorganic ions ( $\text{Ca}^{2+}$ ,  $\text{Cl}^-$ ,  $\text{Fe}^{2+}$ ), which are known to promote inorganic fouling of the FO membrane, was examined.

Experimental work was divided into three parts. The first part focused on the optimization of EC parameters through preliminary experiments (using synthetic SGPW) and Response Surface Methodology (RSM) optimization (using industrial SGPW). The second part explored COD and ion removal efficiency upon the addition of a coagulant aid to EC while the third part analyzed fouling reduction in FO after feed pretreatment. A comparison of contaminant removal and flux in FO for chemical coagulation pretreatment of SGPW was also performed.

In the first part, better COD removal (but lower ion removal) was observed under RSM's optimum conditions (pH 3.2, time = 35 mins and current density =  $45 \text{ A/m}^2$ ) compared to the neutral pH condition from preliminary experiments (pH 7, time = 40 mins and current density =  $200 \text{ A/m}^2$ ). The addition of 25 ppm polyacrylic acid (PAA) under neutral pH condition improved COD and ion removal significantly due to the stretched out conformation of polymer and its lesser adsorption propensity. COD, chloride, calcium and iron removals were 69.78%, 52.49%, 36.64% and 61.33% respectively. SGPW pretreatment via EC, prior to FO, led to a 27-37% reduction in flux compared to a 70% flux decline for raw SGPW feed. Final flux at 450 minutes for acidic pH (with no PAA) and neutral pH (with 25 ppm PAA) pretreatments were 3.53 and 5.22 LMH, respectively. COD and ion removal was least when 3000 ppm of alum was employed; however, no significant gypsum fouling (thus higher flux) was observed in FO

due to slow nucleation and increased gypsum solubility in the presence of high concentrations of competing ions like magnesium and sodium. Acidic pH condition (with no PAA) is recommended for EC pretreatment of SGPW if only generation of reusable water for fracking operations is required. However, if higher product water quality is needed and secondary membrane treatment can be employed, neutral pH condition (with 25 ppm PAA) is recommended.

## **Acknowledgement**

I would like to thank God for His support and guidance in my life, particularly for giving me strength throughout the course of this project. I would also like to acknowledge and express my sincere gratitude to my supervisor, Dr. Saifur Rahaman, who encouraged me and gave very helpful suggestions that enabled the completion of this project. I would also like to thank Steve Glavac at Cambrium Energy for providing wastewater samples upon request. I appreciate the analytical help from Hong Guan (lab technician, Concordia University) and also, the contribution of all members of the Rahaman research group.

## Table of contents

List of Tables.....	viii
List of Figures.....	ix
List of Abbreviations.....	xi
Chapter 1 – Introduction.....	1
1.1 Hydraulic Fracturing Overview.....	1
1.2 Motivation.....	2
1.3 Objectives and Scope of Thesis.....	4
1.4 Organization of Thesis.....	5
Chapter 2 - Literature Review.....	7
2.1 Environmental Issues and Regulations in the United States.....	7
2.2 Environmental Issues and Regulations in Canada.....	9
2.3 Current Technologies for SGPW Treatment.....	9
2.3.1 Biological process.....	10
2.3.2 Physical and chemical processes.....	10
2.3.3 Membrane processes.....	10
2.3.4 Industrially employed technologies.....	10
2.3.5 Combined technologies.....	11
2.4 EC for SGPW treatment.....	12
2.4.1 Improvement of EC through coagulant aid addition.....	12
2.5 Forward Osmosis for high salinity wastewater treatment.....	13
2.6 Mechanism, Advantages and Disadvantages of EC and FO processes.....	15
2.6.1 Electrocoagulation.....	15
2.6.2 Forward Osmosis.....	19
Chapter 3 - Preliminary and Response Surface Methodology Experiments for Optimization of Parameters.....	24
3.1 Introduction.....	24
3.2 Materials and Methods.....	25
3.2.1 Materials.....	25
3.2.2 Methodology.....	27
3.2.3 Analytical Methods.....	31
3.3 Results and Discussion.....	31
3.3.1 Preliminary experiments.....	31

3.3.2 RSM experiments .....	35
3.3.3 Energy and Electrode consumption .....	47
3.4 Conclusions .....	48
Chapter 4 – Effect of Coagulant Aid Addition on COD and Ion Removal in Hydraulic Fracturing Wastewater.....	50
4.1 Introduction .....	50
4.2 Materials and Methods .....	50
4.2.1 Materials .....	50
4.2.2 Methodology.....	51
4.3 Results and Discussion .....	52
4.3.1 Nonionic Polyacrylamide (nPAM).....	52
4.3.2 Polyacrylic Acid (PAA) .....	53
4.4 Sludge Production .....	57
4.5 Conclusions .....	58
Chapter 5 – Fouling Reduction Analysis in Forward Osmosis Experiments .....	60
5.1 Introduction .....	60
5.2 Materials and Methods .....	60
5.2.1 Materials .....	60
5.2.2 Experimental setup .....	60
5.2.3 Methodology.....	61
5.2.4 Analytical Methods .....	62
5.3 Results and Discussion .....	62
5.3.1 Chemical Coagulation Dosage Optimization .....	62
5.3.2 Average flux for different feed streams.....	63
5.3.3 Membrane Analysis.....	69
5.4 Conclusions .....	70
Chapter 6 - Conclusions and Recommendations.....	72
References .....	75

## List of Tables

Table 3.1 - Synthetic wastewater composition for preliminary experiments .....	24
Table 3.2a - Produced water quality analysis (June 2015) from an unconventional oil and natural gas extraction field in Western Canada. Reported TDS = 174,591 mg/L and salinity = 17.64%.....	25
Table 3.2b - Laboratory analysis of industrial wastewater for specific contaminants .....	26
Table 3.3a - Variables and their coded values for Central Composite Design.....	27
Table 3.3b - Design of Experiments for three variables: pH, current density and time ...	28
Table 3.4 - Preliminary experiment results .....	30
Table 3.5 - Design of twenty (20) experiments: variables and the corresponding experimental and predicted responses .....	34
Table 3.6 - COD and ion removals under preliminary and optimized conditions.....	45
Table 4.1 - Contaminant removal in SGPW under optimized RSM conditions .....	52
Table 4.2 - Contaminant removal in SGPW under preliminary experiment conditions ...	53
Table 4.3 - Sludge generation analysis.....	56
Table 5.1 - Porifera's TFC membrane specifications .....	59
Table 5.2 - Turbidity and COD reduction for different alum concentrations.....	61
Table 5.3 - Initial and final flux data for 450 minutes of FO operation .....	62
Table 5.4 - Conductivities of initial draw and feed solutions.....	63
Table 5.5 - Contaminant removal after chemical coagulation and EC treatment under two different pH conditions.....	64
Table 6.1 - Desired water quality for hydraulic fracturing .....	73

## List of Figures

Figure 1.1-1 - Water Usage and Consumption in the Fracking Process .....	2
Figure 2.1-1 - Pathways for water and air contamination due to well leakage and poor (or lack of) wastewater treatment prior to storage or disposal .....	7
Figure 2.6-1 - Laboratory schematic for Electrocoagulation process .....	14
Figure 2.6-2 - Contaminant removal mechanisms in an EC reactor (cathode in this research was not inert).....	16
Figure 2.6-3 - Schematic of Forward Osmosis operation (no heating was applied since experiments are done at room temperature) .....	18
Figure 2.6-4 - FO laboratory setup .....	19
Figure 2.6-5 – Osmotic pressure vs Concentration analysis for prospective Draw solutes in the FO process .....	22
Figure 3.1 - EC laboratory setup .....	25
Figure 3.2 - Voltage increments over time for different electrode distances.....	31
Figure 3.3 - Voltage increments over time for different current densities .....	32
Figure 3.4- Cathode passivation on Fe electrode after 60 min.....	33
Figure 3.5 - pH trend for different electrode distances .....	33
Figure 3.6 - Color changes of SGPW during EC .....	35
Figure 3.7 - %Fe removal contour plots describing interactions between a) time and pH, b) current density and pH, and c) current density and time.....	36
Figure 3.8 - Main effects plot for iron removal showing mean removal for a) incremental pH changes, b) incremental time, and c) incremental current densities.....	37
Figure 3.9 - %Ca removal contour plot describing interactions between a) time and pH, b) current density and pH, and c) current density and time.....	38
Figure 3.10 - Main effects plot for iron removal showing mean removal for a) incremental pH changes, b) incremental time, and c) incremental current densities.....	40
Figure 3.11 - %Cl <sup>-</sup> removal contour plot describing interactions between a) time and pH, b) current density and pH, and c) current density and time.....	41
Figure 3.12 - %Cl <sup>-</sup> removal contour plot describing mean removal for a) incremental pH changes, b) incremental time, and c) incremental current densities.....	42
Figure 3.13 - %COD removal contour plot describing interactions between a) time and pH, b) current density and pH, and c) current density and time.....	43
Figure 3.14 - %COD removal main effects plot describing mean removal for a) incremental pH changes, b) incremental time, and c) incremental current densities.....	44
Figure 4.1 - Molecular structure of a) polyacrylic acid and b) nonionic polyacrylamide (Sigma-Aldrich).....	49
Figure 4.2 - New SGPW (left) and old SGPW (right) .....	50

Figure 4.3 - COD removal % over time with and without nPAM .....	51
Figure 4.4 - Contaminant removal in Batch 1 and 2 samples under neutral pH showing improved removal upon PAA addition .....	54
Figure 4.5 - PAA conformations under acidic (pH 4) and neutral pH (pH 7).....	55
Figure 4.6 - Contaminant removals at pH 7 and pH 3.2 for Batch 2 samples (without PAA).....	55
Figure 5.1 - Flux trend over 450 minutes of operation for different feed streams.....	62
Figure 5.2 - Graphical comparison of COD and ion removal in EC and alum pretreatment .....	65
Figure 5.3 - Mechanism of gypsum scale formation (although figure describes scale formation on a nanofiltration membrane, mechanism is also applicable to FO membrane) .....	66
Figure 5.4: (a) SEM for virgin TFC membrane; Fouling observations on TFC membrane (b) when raw SGPW was employed as feed; (c) when SGPW, treated via EC at pH 3.2, time 35 mins and current density 45 A/m <sup>2</sup> , was employed as feed; (d) when SGPW, treated via EC at pH 7, time 40 mins and current density 200 A/m <sup>2</sup> with PAA, was employed as feed. ....	69

## List of Abbreviations

AC	Alternating Current
ANOVA	Analysis of Variance
A	Anode Material
BAF	Biological Aerated Filter
BOD	Biological Oxygen Demand
C	Cathode
CTA	Cellulose Triacetate
COD	Chemical Oxygen Demand
DI	Deionized
DRBC	Delaware River Basin Commission
DC	Direct Current
DOC	Dissolved Organic Carbon
EC	Electrocoagulation
ED	Electrodialysis
EDAX	Energy Dispersive X-ray Spectroscopy
FO	Forward Osmosis
FO-MBC	Forward Osmosis-Membrane Brine Concentrator
HClO	Hypochlorous Acid
ICP	Internal Concentration Polarization
LMH	Liters per meter square per hour
LPM	Liters per minute
M	Molar Concentration
MF	Microfiltration
NF	Nanofiltration
nPAM	Nonionic Polyacrylamide
OPUS	Optimized Pretreatment and Unique Separation
PAA	Polyacrylic Acid

PAC	Powdered Activated Carbon
PRO	Pressure Retarded Osmosis
RO	Reverse Osmosis
RSM	Response Surface Methodology
RSF	Reverse Salt Flux
S	Structural Parameter
SEM	Scanning Electron Microscopy
SGPW	Shale Gas Produced Water
SRBC	Susquehanna River Basin Commission
TDS	Total Dissolved Solids
TFC	Thin Film Composite
TMP	Trans-Membrane Pressure
TOC	Total Organic Carbon
TSS	Total Suspended Solids
UF	Ultrafiltration

## **Chapter 1 – Introduction**

### **1.1 Hydraulic Fracturing Overview**

Hydraulic Fracturing, also known as fracking, is a technique that is increasingly applied for unconventional oil and gas extraction. Prior to the implementation of hydraulic fracturing, oil and gas was extracted conventionally with the use of vertical drilling in oil reserves. However, oil and gas, locked in low permeability formations such as shale gas beds and tight sandstones, could not be exploited. Hydraulic fracturing has thus enabled access to these formations, enhanced oil and gas productivity and reduced the market prices of oil and gas<sup>1,2</sup>.

For unconventional oil and gas to be extracted from a formation, horizontal drilling is first performed. Wells are bore several kilometers downward depending on the depth of the oil and gas bed and up to two kilometers horizontally<sup>3</sup>. A steel casing is inserted as an intermediate protection to prevent leakage through the well. Between the steel casing and well is a cement filling to further enhance well integrity<sup>4</sup>. After these protective steps, hydraulic fracturing is employed. Fluids are pumped into wells at high pressure in order to fracture or crack the formation and enable the permeation of oil and gas into the wells and eventually, to the surface. The fluids typically consist of water, sand and other chemical additives such as hydrochloric acid to hinder iron precipitation and guar gum to promote fluid transport<sup>4</sup>. The water volume consumed depends on the type of formation, among other factors<sup>5</sup>. About 2-20 million gallons of water (or more), typically from fresh water sources, are consumed per well. Generally, as oil and gas migrates to the surface, some additional volume of water, local to the formation, is also given off<sup>6</sup>. This additional volume of water is often referred to as produced water.

*Figure 1.1-1* below describes the different stages of water usage and generation in the fracking process.

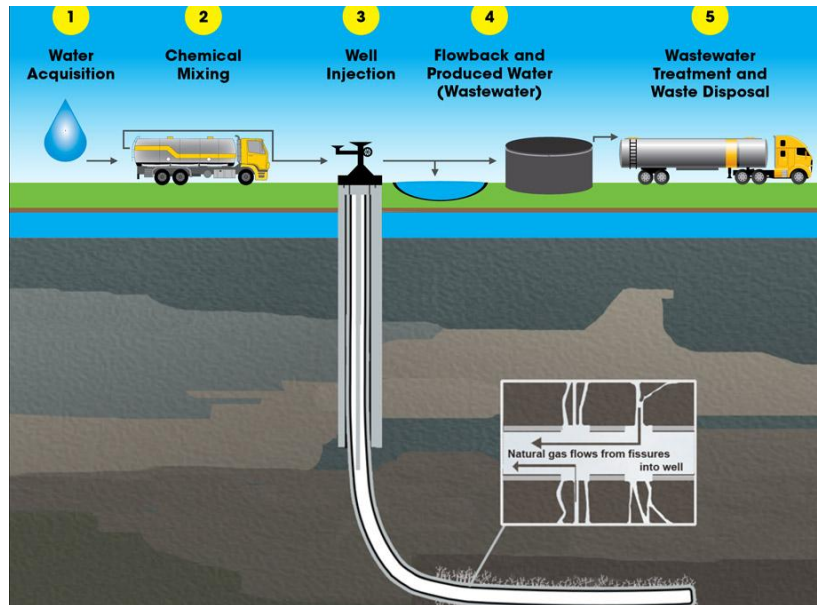


Figure 1.1-1: Water Usage and Generation Stages in the Fracking Process<sup>7</sup>

Produced water is often used interchangeably with flowback water, but both slightly differ from each other. Produced water is generated over the life cycle of the well while flowback water is generated during the first few weeks of well operation. In addition, flowback water comprises mainly of chemical additives and sand that were initially pumped into the well. It might also contain some saline water from the formation. Produced water, on the other hand, is predominantly highly saline water local to the formation and the salt composition varies depending on the geology of the formation<sup>3</sup>.

## 1.2 Motivation

Zhao et al<sup>8</sup> state that the volume of wastewater released from one oil field over time exceeds, by 10 times, the amount of extracted hydrocarbon. Considering the rising application of hydraulic fracturing, it is certain that greater amounts of produced water will be generated while fresh water sources continue to be depleted. To protect fresh water sources and the environment, strict governmental regulations regarding disposal (*Section 2.1 – 2.2*) have been developed. These regulations vary depending on the region and ultimately, the goal is to promote wastewater reuse. Since in many cases the generated wastewater cannot be directly re-used, several companies are exploring

wastewater treatment as a viable option, as it decreases the demand on the fresh water sources, disposal problems and overall cost of the process. Typically, the salinity and final fate of produced water determine whether or not more than one treatment option will be applied. One company, Encana, currently employs the use of filters, chemical treatment and reverse osmosis to decrease the TDS levels of its produced water to that of drinking water, which is typically below 250 ppm<sup>9,10</sup>.

Suitable pretreatments such as evaporation, coagulation, chemical precipitation, filtration and sedimentation have been employed to enable re-use<sup>9</sup>. However, the disadvantages of these pretreatment techniques include specificity in contaminant removal (in the case of chemical precipitation), excessive use of additional chemicals and overall inefficiency for effective contaminant reduction. It is therefore crucial to find and optimize a suitable pretreatment technology that overcomes the limitations of conventional pretreatment practices employed industrially.

Electrocoagulation (EC) is a promising pretreatment technology that can be employed for highly saline produced water. EC involves the use of electrode materials such as aluminum and iron, which are connected to a current supply, for the generation of ionic species that function as coagulants for contaminant removal in an aqueous solution<sup>11</sup>. Regardless of the anode material, when current is applied, the anode material (A) dissolves in the solution, forming  $A^{n+}$ . Reactions at anode and cathode (C) are described below<sup>11,12</sup>:



EC is a very advantageous process in that it is nonspecific in its treatment (meaning that it can remove multiple contaminants in one run) and it incorporates oxidation, coagulation and precipitation, all of which are otherwise being employed individually in conventional wastewater treatment. After pretreatment, Forward Osmosis (FO) can be applied for further desalination and SGPW treatment. FO employs the principle of osmosis, a natural phenomenon that drives the movement of water from regions of low salt concentration to regions of high salt concentration in the presence of a semi-permeable membrane<sup>13</sup>. As a membrane process and due to the high salinity of SGPW,

FO can suffer from fouling due to precipitation of inorganics; hence, it is necessary to optimize the pretreatment process in order to reduce inorganics concentration in SGPW.

### **1.3 Objectives and Scope of Thesis**

The overall objective of this thesis is to investigate the improvement of the forward osmosis process by fouling reduction through the application of electrocoagulation as a pretreatment for high salinity SGPW. No study has been done on combining EC and FO for fracking wastewater treatment, although studies have been conducted on the individual processes for fracking wastewater treatment. Electrocoagulation is applied as a pretreatment for the removal of turbidity, chemical oxygen demand (COD) and specific ions (calcium, iron and chloride), which have been reported to cause inorganic fouling of the FO membrane. COD consists of both organic and inorganic substances that can be chemically oxidized in the wastewater. Although it is not a distinct pollutant, COD is typically employed as a measure of the effectiveness of a treatment process<sup>14</sup>. Calcium ions can precipitate and clog pipelines while chlorides and iron can lead to pipeline corrosion. Concentrations of COD and the aforementioned ions are high in SGPW and thus limit reuse of wastewater. They also lead to scale formation on the FO membrane and hinder the effectiveness of the application of FO treatment alone. Therefore, reducing their concentration is essential to promote reuse and recycling of wastewater for oil and gas extraction. There was no target removal percentage for these contaminants; rather, EC was examined to observe how much of these ions and COD it can remove. The list below was explored in this research in order to achieve the overall objective:

1. Optimization of EC parameters through preliminary one-factor-at-a-time experiments and response surface methodology (RSM) experiments - Preliminary one-factor-at-a-time experiments analyzed the effect of different EC parameters on turbidity removal alone. The goal was to determine range of values for each EC parameter that produced the best turbidity removal. One-factor-at-a-time experiments do not however take into account the effect of the interaction among EC parameters on contaminant removal. As a result, RSM experiments were employed not only to observe the effect of the interaction among the chosen

parameters, but also to identify which parameters are significant in the removal of a specific contaminant.

2. Investigation of the effect of the addition of a coagulant aid to EC for improved treatment of fracking wastewater - This aspect has not been investigated for SGPW treatment; hence, results will be beneficial for treatment optimization of such highly saline wastewater. Coagulant aids are known to help in settling of flocs, thus improving contaminant removal<sup>15</sup>. An anionic organic coagulant aid was selected because organic polymers were reported to be better than inorganic polymers due to lower cost, biodegradability, less generated sludge, and low dosage for effective treatment<sup>16</sup>. Furthermore, anionic and nonionic polymers are more advantageous since they are less toxic than cationic polymers<sup>16</sup>. A nonionic polymer was also selected to compare with the anionic polymer.
3. Analysis of flux decline in FO experiments – FO was conducted with different feed solutions – raw SGPW, EC-pretreated feed solutions (with and without coagulant aid) and chemically coagulated wastewater. Water flux was compared and membrane analysis was performed to observe membrane structure after treatment of each feed stream.

This thesis does not cover draw solution regeneration, sludge disposal or treatment.

#### **1.4 Organization of Thesis**

This thesis is divided into the following chapters:

- Chapter 1 – Introduction to the hydraulic fracturing process, motivation of research, thesis objectives and organization
- Chapter 2 – Literature review on fracking environmental issues and regulations, current treatment technologies, EC and FO research that have been conducted for shale gas produced water
- Chapter 3 – Preliminary Experiments and Response Surface Methodology Analysis for the Optimization of Electrocoagulation Parameters
- Chapter 4 – Effect of Coagulant Aid Addition on Contaminant Removal in the Electrocoagulation process

- Chapter 5 – Fouling Reduction Analysis in Forward Osmosis Experiments
- Chapter 6 – Conclusions and recommendations

## **Chapter 2 - Literature Review**

High salinity of SGPW and the corresponding environmental effects resulting from disposal have led to the imposition of strict regulations on fracking operations.

### **2.1 Environmental Issues and Regulations in the United States**

In the United States, the application of hydraulic fracturing has greatly increased productivity in the oil and gas sector. States like Texas, Oklahoma, and Colorado employ this technique for oil and gas exploration. However, over the years, concerns have been raised due to the adverse impacts of the process on the environment. Firstly, hydraulic fracturing can result in groundwater contamination through leakage from injection wells, drilling wells or storage ponds. Salts and other soluble contaminants could escape from the well and migrate to shallow aquifers, leading to higher than acceptable levels of contaminants in groundwater. Vengosh et al<sup>17</sup> highlight the case of Garfield County, CO where higher levels of chloride were observed in drinking water and this trend was in line with the corresponding increase in oil and gas exploration in the region. Stray gas can also contaminate groundwater. Particularly, the occurrence of elevated levels of methane in groundwater wells near hydraulic fracturing sites has been reported in some studies<sup>17,18</sup>. The major challenge here is in identifying the source of methane especially if the exploration zone already has some naturally occurring methane<sup>19</sup>. Another possible site of contamination is surface water due to spills or leaks while transporting produced water samples to disposal wells and ponds<sup>3,17</sup>.

Many states in the US are water-stressed and limited fresh water availability causes competition between hydraulic fracturing operations and other industries such as agriculture and mining that also require a large amount of water for their operations. The resulting environmental effects include threats of desertification and drought<sup>5,20,21</sup>. Lastly, well operators prefer to dispose their wastewater by deep well injection due to costs associated with treatment. However, this disposal method has been speculated to induce seismicity. Accidental spills and eventual contamination of surface (and ground) water are also prone to occur<sup>22</sup>.

*Figure 2.1-1* below illustrates different possible pathways of contamination resulting from hydraulic fracturing operations.

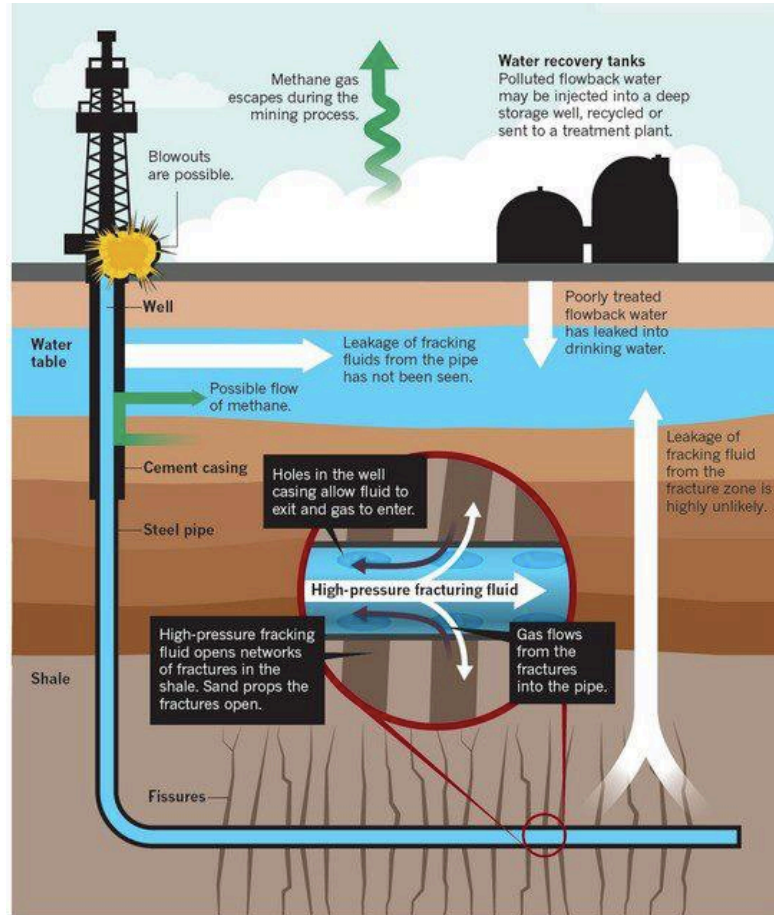


Figure 2.1-1: Pathways for water and air contamination due to well leakage and poor (or lack of) wastewater treatment prior to storage or disposal<sup>23</sup>

In the US, each state manages its legislation on hydraulic fracturing operations<sup>17</sup>. For example, the state of Pennsylvania decided to discontinue the treatment of produced water in municipal wastewater treatment plants. The reason was mainly because these plants were not able to reduce the salinity of fracking wastewater to the required total dissolved solids (TDS) threshold of 500 mg/L and the “treated” effluent ended up in surface waters<sup>24,25</sup>. Also, other commissions, municipalities and water regulatory bodies that are influenced by fracking operations can impose additional regulations. For example, in the Marcellus shale region, the Susquehanna River Basin Commission (SRBC) imposed restrictions on amount of water that can be withdrawn for fracturing purposes. In Delaware, the Delaware River Basin Commission (DRBC) prohibited any

form of drilling operations. Such regulations have reportedly led to an increase in the exploration of reuse and recycling options such as wastewater treatment<sup>26,27</sup>.

## **2.2 Environmental Issues and Regulations in Canada**

In Canada, provinces like British Columbia, Alberta, Saskatchewan, Manitoba, Northwest Territories and some parts of Quebec accept shale gas exploration. Other provinces - Ontario, New Brunswick, Nova Scotia, Prince Edward Island, Newfoundland and Labrador - either have a ban or moratorium on fracking operations. Yukon's acceptance of fracking is not clear. In Quebec, legislation had hindered shale gas exploration in the lowlands of the St. Lawrence River. However, in 2016, three fracking operations were recently permitted on Anticosti Island<sup>28</sup>.

Environmental issues in Canada, resulting from hydraulic fracturing operations, are similar to those in the US. Also, each province manages its own fracking regulations. For example, Montney basin encompasses part of the northeast of British Columbia and the northern part of Alberta and it spans about 130,000 km<sup>2</sup>. It generates about 10-25 million liters of water per well and the province of British Columbia requires well operators to have a water management plan<sup>9</sup>. In New Brunswick, prior to the indefinite ban on hydraulic fracturing in the region, well operators were required to have a strategy for managing water use<sup>29</sup>. For hydraulic fracturing companies, wastewater treatment and reuse is a growing trend that is both sustainable and economic for water management.

## **2.3 Current Technologies for SGPW Treatment**

Several researchers have explored the feasibility of different technologies as pretreatment options for shale gas produced water. Guerra et al<sup>30</sup> examined different technologies (biological, physical, membrane and industrially employed processes) that have been applied for the treatment of SGPW. The authors considered various factors such as contaminant removal, mobility, and footprint. Igunnu et al<sup>31</sup> also conducted a similar study for conventional oil and gas produced water.

### **2.3.1 Biological process**

A biological aerated filter (BAF) is one technology that has been employed and pollutants like oil, nitrogen, iron, heavy metals, COD and biological oxygen demand (BOD) have been successfully removed. However, BAF has a large footprint, is immobile and requires extensive post treatment. It also does not decrease TDS and high salt concentration ( $Cl^- > 6600 \text{ mg/L}$ ) is toxic for indigenous microbes.

### **2.3.2 Physical and chemical processes**

For particulate removal, hydrocyclones, centrifuge, and API gravity separators have been used. The major disadvantage however is that these technologies only target removal of one contaminant, but do not address TDS reduction. Physical and chemical processes such as oxidation, adsorption and granular activated carbon fluidized bed reactors have also been utilized for total organic carbon (TOC), oil and grease and some metal removal. The drawback is mainly the cost of adsorption media and regeneration by thermal means.

### **2.3.3 Membrane processes**

SGPW has been treated using membrane processes such as RO, microfiltration (MF), ultrafiltration (UF), nanofiltration (NF) and electrodialysis (ED). MF, UF and NF are typically effective for particulate and dissolved organics removal. RO can remove metals, but it is not suitable for highly saline wastewater ( $TDS > 40,000 \text{ ppm}$ ) due to the high operating pressure requirement. ED showed poor removal of organics and non-conductive substances like organics, and precipitate-forming elements such as calcium and magnesium need to be removed prior to ED process. Otherwise, they will foul the ion exchange membrane.

### **2.3.4 Industrially employed technologies**

Veolia's optimized pretreatment and unique separation (OPUS) technology combines chemical softening, filtration and ion exchange as pretreatment prior to RO operated at high pH. The chemical softening process however consumes a large volume of chemicals and also, for longer use of the ion exchange resins, contaminants have to be

in low concentration. Otherwise, resins will have to be replaced frequently and this will render the technology uneconomical. Also, Oasys<sup>32</sup> developed a Membrane Brine Reactor for high salinity produced water that has been pretreated using a chemical oxidizer, caustic soda and soda ash for precipitation of inorganics. Filtration using a greensand media is then employed for removal of iron and particulate matter. Resulting effluent is passed through a cartridge filter before entering the membrane brine reactor for further treatment. It is evident that pretreatment stages are both capital and resource intensive due to cost of chemicals and regeneration of filtration media.

### **2.3.5 Combined technologies**

Fakhru'l-Razi et al<sup>33</sup> highlight different processes for conventional oil and gas produced water treatment. One combined process utilizes pH adjustment, aeration and a separation unit as pretreatment prior to sand filtration for metal removal. Another involves the use of oil/water separator, microfiltration, and activated carbon prior to RO. Although the latter process can generate effluent with TDS levels below 250 mg/L, the multiple pretreatments per process elevate the treatment and operational costs; thus making the technology uneconomical.

Cho et al<sup>34</sup> specifically examined the application of microbubbles and filtration as pretreatment for SGPW prior to membrane distillation treatment. Real and synthetic produced water were used in their study and the TDS level of the real produced water from two shale gas basins in the US was greater than 350,000 mg/L. The implementation of microbubble pretreatment was however not effective for TDS reduction, but it could only reduce turbidity. There was no significant improvement in the quality of the wastewater as turbidity decline was minimal. As a result, scale formation contributed considerably to flux decline in the membrane distillation process. Also, the high-pressure requirement for microbubble pretreatment adds to the capital and operational cost of the pretreatment process.

Wang et al<sup>35</sup> investigated the use of chemical coagulation for pretreating SGPW and further treatment using wet air oxidation process. Polyaluminium chloride and anionic polyacrylamide were used as flocculants and only 8.2% COD removal was

achieved. Also, chemical coagulation requires the addition of a large amount of chemicals, which increases the cost of the pretreatment process.

Rosenblum et al<sup>36</sup> also examined the effectiveness of coagulation combined with powdered activated carbon (PAC) for turbidity, polyethylene glycol, total petroleum hydrocarbon, and dissolved organic carbon (DOC) reduction in unconventional oil and gas produced water. 1000 ppm of PAC was used and this resulted in only 14.6% DOC reduction for wastewater from a horizontally fractured well. The low contaminant removal and the high cost of PAC limit the practical application of this method.

## **2.4 EC for SGPW treatment**

Published research exploring EC treatment of SGPW is not voluminous. Zhao et al<sup>8</sup> explored the application of EC as pretreatment prior to RO for conventional oil and gas produced water. EC showed very good removal for turbidity, COD and hardness and unlike chemical coagulation, coagulants are generated in-situ and it can handle several pollutants in one tank. For these reasons, EC can function as a better pretreatment process compared to chemical coagulation. In their work, initial COD and hardness (as CaCO<sub>3</sub>) of the wastewater were 280 mg/L and 300 mg/L respectively and removals for both reached 66.64% and 85.81% respectively.

Lobo et al<sup>37</sup> studied the combination of alternating current (AC)-powered EC and granular biochar for SGPW treatment. Wastewater was gotten from the Denver-Julesburg basin in the US. pH and COD was about 7 and 3600 ppm, respectively. COD removal was around 5% with biochar after 30 min and 14% without biochar after 50 min. Low COD and TDS removal was reported in this work and the authors concluded that additional research is needed to optimize contaminant removal.

### **2.4.1 Improvement of EC through coagulant aid addition**

Addition of coagulant aids in order to improve contaminant removal efficiency is another research area that has also been studied for different types of wastewater except SGPW. Coagulant aids are known to improve settling process by increasing floc density<sup>15</sup>. Haydar et al<sup>38</sup> studied chemical coagulation treatment of tannery wastewater by applying alum as coagulant and two types of coagulant aids - cationic and anionic

polymers. A part of their work focused on observing the effect of coagulant aid on contaminant removal. Initial COD was 2442 mg/L and pH was 8.98. The addition of coagulant aid improved chromium removal and reduced sludge volume. Aguilar et al<sup>39</sup> also report reduced sludge volume when coagulant aids are used in chemical coagulation process. Haydar et al concluded that although coagulant aids significantly decrease sludge production, the effluent COD is still relatively high. As a result, they highlighted the need for further treatment to reduce COD levels.

Un et al<sup>40</sup> observed the contrary in terms of the COD removal efficiency when polyaluminium chloride was used as coagulant aid during EC operation. The addition of a coagulant aid led to better COD removal within a short period of time. In their work, the wastewater was oily and acidic (pH = 1.4) with COD of 15,000 ppm. EC was employed with aluminum electrodes at different pH, current density and coagulant aid dosage. Optimum removals were seen after 90 mins at pH 7, 350 A/m<sup>2</sup> current density and 500 mg/L polyaluminum chloride.

Irfan et al<sup>41</sup> observed low COD removals (10-19%) and about 50% TSS removal when alum and polyaluminum chloride were used for treating pulp and paper mill wastewater. Nevertheless, when anionic polyacrylamide (anionic polymer) was added, COD and TSS removals increased to about 78% and 96% respectively at acidic pH. Aguilar et al<sup>42</sup> also observed improved TSS removals in their work and concluded that the addition of coagulant aids improved particle removal efficiency.

## **2.5 Forward Osmosis for high salinity wastewater treatment**

Research has also been conducted on the application of forward osmosis for treating SGPW or highly saline wastewater. Roy et al<sup>43</sup> examined FO treatment of saline wastewater generated from contaminated soil. Porifera's proprietary membrane was used and water flux decline from 19.7 LMH to 2 LMH was observed. This decline was attributed to the reduced osmotic pressure and RSF during the process. Bell, E.A.<sup>44</sup> also investigated the performance of FO for treating saline SGPW for three weeks continuously. TFC and CTA were used and water flux and RSF for the two membranes were observed. For the TFC membrane, Bell observed that RSF increased and fouling was more pronounced, despite the hydrophilicity and smoothness of the membrane

surface. The author linked this high fouling propensity to the morphology of the TFC membrane since its active layer contains carboxyl ( $-\text{COOH}$ ) and amide ( $-\text{NH-CO}$ ) groups that can form hydrogen bonds with contaminants. The author also mentioned that the high initial water flux contributed to fouling since it causes the attraction of more contaminants to the membrane surface and compresses the cake layer. The high initial flux however declined over time due to concentration polarization. Major foulants observed on the membrane were hydrocarbons and ions such as iron, chloride, calcium and sodium.

Zhao et al<sup>45</sup> studied the effect of different operating conditions such as temperature, cross flow velocity and salinity of the feed solution on FO performance. As expected, increasing the feed salinity decreased the initial and final water flux of the system. Nevertheless, the authors argued that raising the cross flow velocity (from 5cm/s to 10cm/s), in spite of high feed and draw solution salinity, can lead to higher water flux due to reduced concentration polarization.

Hickenbottom et al<sup>46</sup> investigated the treatment of drilling mud wastewater through FO. CTA membrane was used in their study and the draw solution was concentrated sodium chloride (260 g/L). The authors reported an initial flux of 14 LMH, which later decreased to about 2 LMH. It was also observed that increasing the cross flow velocity (in their case, from 0.075 m/s to 0.03 m/s) reduced the rate of flux because higher velocity scours the membrane. In terms of solute migration from feed to draw side, no migration of major ions like calcium, iron and magnesium was observed.

Industrially, FO has also been applied for the treatment of SGPW with and without pretreatment. Shaffer et al<sup>47</sup> examined different draw solutions that have been employed for improved performance of the FO system for SGPW treatment. The authors highlighted the implementation of an FO system that used ammonia-carbon dioxide as draw solute for treating SGPW (TDS = 73,000 mg/L) from Marcellus shale. Water flux declined to about 3 LMH for this system.

Also, Coday et al<sup>48</sup> reported FO pilot tests for SGPW treatment, which employed a forward osmosis-membrane brine concentrator (FO-MBC). The wastewater was first pretreated using an oxidizer, caustic soda (NaOH) and soda ash ( $\text{Na}_2\text{CO}_3$ ) and pretreated wastewater was passed through the FO membrane and becomes concentrated in the

MBC. The FO-MBC utilizes ammonium bicarbonate and ammonium hydroxide in water as draw solution. In the first pilot test, 60,000 gallons of SGPW from Marcellus basin was pumped through the FO-MBC for 800 h. The average flux reported was around 2-3 LMH. 40,000 gallons from another basin was tested for 400 h. Initial TDS of wastewater from this basin before and after treatment is about 103,000 mg/L and 737 mg/L, respectively. Average water flux was about 3 LMH.

Lastly, Coday et al<sup>49</sup> studied the significance of operating conditions and membrane selection on the efficiency of the FO process. SGPW was used and the system was run in osmotic dilution mode. Different operating conditions such as cross flow velocity and membrane packing were tested and the authors stated that operating conditions were more significant in their effect on the FO process. They also highlighted the importance of a suitable pretreatment in order to reduce long-term fouling of the system, as they stated that long-term fouling, after cake layer is formed, is mainly dependent on interactions among foulants on membrane surface.

## **2.6 Mechanism, Advantages and Disadvantages of EC and FO processes**

### **2.6.1 Electrocoagulation**

EC is an electrolytic process during which oxidation and reduction occur at the anode and cathode respectively upon the application of current. It combines the following stages in its operation – electrolysis, coagulant formation through anode dissolution, contaminant-coagulant interaction and flotation for the removal of by-products<sup>50</sup>. A typical laboratory EC system consists of a beaker with an appropriate volume of wastewater to be treated, magnetic stirrer, a stir bar, anode and cathode electrode materials, and a power supply (*Figure 2.6-1*).

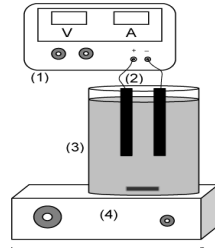
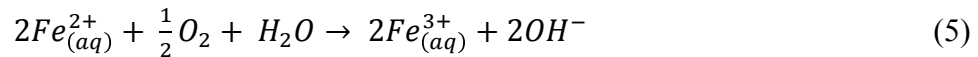


Figure 2.6-1: Laboratory schematic for Electrocoagulation process<sup>51</sup>

Several researchers have investigated contaminant removal efficiency in EC using various types and number of electrodes<sup>12,50,52-55</sup>. Typically, iron and aluminum are used as electrode materials for electrocoagulation due to their efficiency and minimal cost<sup>11</sup>. Nevertheless, other electrode materials like magnesium and stainless steel have also been studied<sup>56-59</sup>. When aluminum is used as the anode<sup>11,12</sup>,  $Al^{3+}$  is formed and when iron is the anode material,  $Fe^{2+}$  is formed, which can be further oxidized to  $Fe^{3+}$ .



Cathode reactions involve the reduction of water to hydrogen gas and hydroxyl ions.



The presence of chlorine and high anode potential leads to the formation of active chlorine agents, which are strong oxidants for organic contaminant removal in wastewater<sup>12</sup>.



The dissolution of the anode, either aluminum or iron, ultimately leads to the formation of aluminum hydroxide ( $Al(OH)_3$ ) and ferric hydroxide ( $Fe(OH)_3$ ). More complex species, monomeric and polymeric, are also generated; however, their existence in the

solution is pH dependent. Hakizimana et al<sup>60</sup> report that soluble anions of aluminum exist at pH <4 and pH>10 while insoluble aluminum hydroxide precipitates exists between pH 4 and 10.

Once these coagulants are formed, contaminant removal from wastewater can occur in three possible ways - charge neutralization; reaction with hydroxyl ions and other cations generated from reactions at the anode, cathode, and in the solution; and ‘sweep coagulation’ through interaction with aluminum or ferric hydroxide<sup>61</sup>.

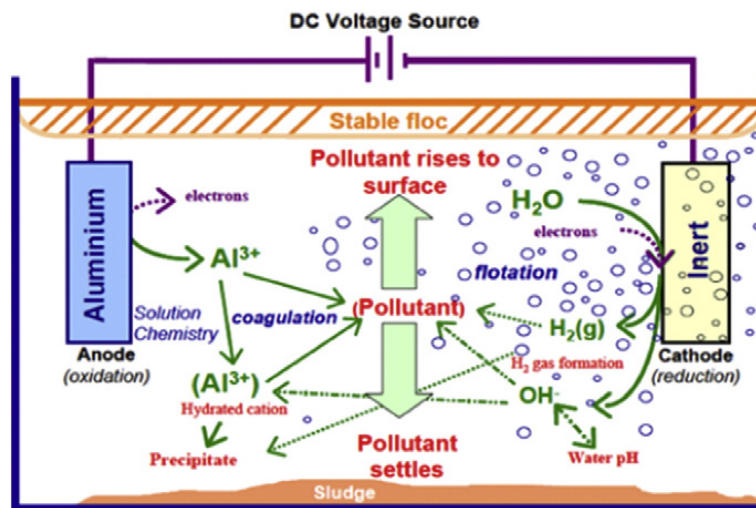


Figure 2.6-2: Contaminant removal mechanisms in an EC reactor<sup>37</sup> (cathode in this research was not inert)

There are several factors that influence the efficiency of EC for contaminant removal – current density, residence time, reactor and electrode design configuration, and wastewater characteristics such as initial pH and conductivity. Current density controls anodic dissolution and the rate of hydrogen gas generation, thus influencing mass transfer and floc formation<sup>60,62</sup>. pH determines which coagulant species and reaction mechanism(s) will dominate in the solution. It also affects adsorption and coagulation<sup>60</sup>. Higher conductivity reduces resistance in the wastewater, residence time for a specific percent removal, and energy requirement for the process. Reactor design includes electrode design and spacing. Hakizimana et al<sup>60</sup> mention that the monopolar parallel spacing (that is, for a four electrode system: Anode-Cathode-Anode-Cathode) results in greater contaminant removal at a low energy cost. Also, decreasing the distance leads to a

reduction in energy consumption, greater mass transfer and thus higher coagulant-contaminant interaction<sup>63</sup>.

Compared to conventional chemical coagulation, EC has the advantage of no excessive chemical addition and lower capital cost. The highly conductive nature of SGPW also decreases the voltage requirement for the EC process, thus reducing electrical and electrode maintenance costs significantly. In addition, Mollah et al<sup>64</sup> state that adsorption interaction between EC-generated hydroxide flocs and contaminants is 100 times better than hydroxides formed via chemical coagulation because hydroxide is generated in situ. EC does not require the addition of chemical coagulants and it has a short reaction and startup time. It also exhibits buffering capacity depending on the initial pH of the treated wastewater. There are several proposed reasons for this buffering effect. If the influent pH is acidic,  $\text{Ca}^{2+}$  and  $\text{Mg}^{2+}$  ions present in the wastewater could displace some  $\text{OH}^-$  ions in  $\text{Al}(\text{OH})_3$ , thus increasing the pH<sup>65</sup>. Also, in a similar manner, if the influent pH is alkaline, calcium and magnesium could consume the hydroxide and form precipitates, thus reducing the pH of the solution. EC is capable of treating different types of wastewater such as oily wastewater<sup>66</sup>, refinery wastewater<sup>67</sup>, and produced water from shale gas operations<sup>37</sup> for the removal of contaminants like oil, ions and heavy metals, and total suspended solids (TSS).

Despite these benefits, just like any treatment process, EC has its drawbacks. Depending on the applied current density, the maintenance requirement of the EC process might be high due to the depletion of the anode. Another problem is cathode passivation, which is the formation of an impermeable oxide layer on the cathode surface. This reduces the transfer of ions from anode to cathode, inhibits anode dissolution, and hence affects coagulant generation in the EC system<sup>68</sup>. It also increases voltage demand and thus energy requirement for the process<sup>69</sup>. The presence of chloride ions however assists in breaking the film through pitting. Around pH 5 and 6, hypochlorous acid ( $\text{HClO}$ ) is dominant while at  $\text{pH} > 6$ , the anions of the acid ( $\text{OCl}^-$ ) are prevalent<sup>62</sup>. If there are organics in the wastewater, the presence of chloride ions could lead to the formation of toxic chlorinated compounds.

In addition, similar to chemical coagulation, sludge generation and disposal is another concern, but sludge generated during EC can be easily separated and dewatered

since it mainly consists of oxides and hydroxides of the anodic material<sup>70</sup>. EC sludge has proven to be a good adsorbent for phosphate removal<sup>71</sup>. Also, the scum and generated sludge can be dried and added to incinerators or boilers as a fuel. After incineration, the ash can be further mixed to fire clay for the creation of firebricks<sup>72</sup>. Another study reported that the incorporation of such ash to clay and Portland cement strengthens the mechanical structure and thermal resistance of these materials<sup>73</sup>.

### 2.6.2 Forward Osmosis

The FO membrane acts as a semi-permeable barrier to permit osmotic flow from feed to draw and hinder salt migration in the same direction. Two membrane orientations are possible: feed facing active layer (FO mode) and feed facing support layer (Pressure retarded osmosis (PRO) mode)<sup>74</sup>. Both positions can be employed depending on the goal of the application of the process. For example, if FO system is needed for power generation, then the PRO mode is appropriate.

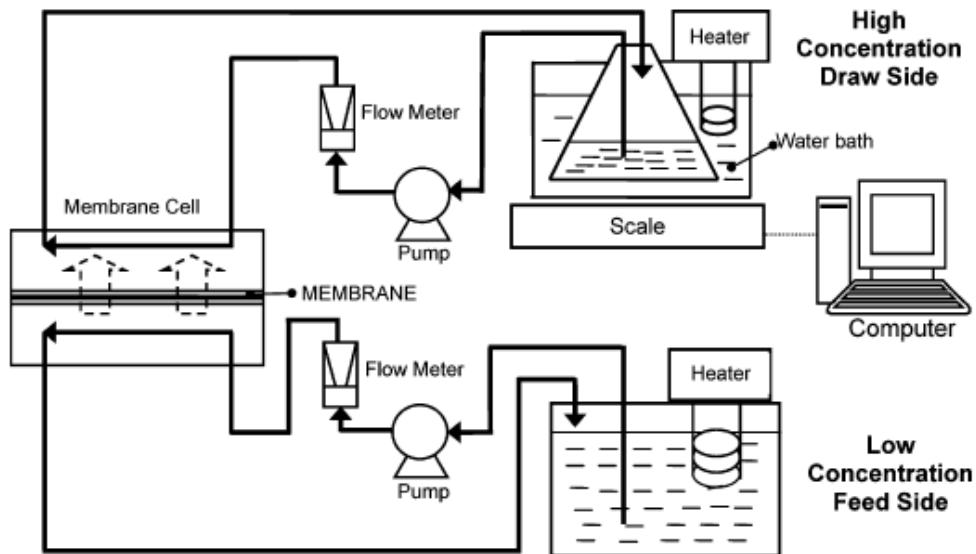


Figure 2.6-3: Schematic of Forward Osmosis operation (no heating was applied since experiments are done at room temperature)<sup>75</sup>

Osmotic pressure difference is the major driving force of the process and it makes FO advantageous than other membrane-based processes. Compared to RO, FO has a lower energy demand and capital cost for its application. Furthermore, FO has shown high contaminant rejection and reduced membrane-fouling<sup>48</sup>. The cake layer on the FO

membrane, caused by contaminants, can be eliminated by osmotic backwashing, which involves the use of deionized (DI) water as the draw solution and the concentrated feed stream as the feed solution. This arrangement reverses the direction of permeate flow, as water will now flow from the draw to feed solution. Consequently, foulants on the feed side of the membrane will be removed and FO fouling can be reversible<sup>76,77</sup>.

FO can be employed for a variety of applications such as high salinity wastewater treatment<sup>48</sup>, seawater desalination<sup>78</sup>, brine concentration<sup>79</sup>, saline soil treatment<sup>43</sup>. For treatment of high salinity wastewater, a draw solution with higher osmotic pressure than the feed is required. If FO is run in osmotic dilution mode, that is, constant draw solution concentration is not maintained throughout the treatment process, the energy cost for draw solution regeneration will be less since the draw solution will be more diluted<sup>80</sup>. Also, several researchers have studied the use of fertilizer-based draw solutions for FO and the resulting diluted draw solution can be directly utilized for irrigation of farmlands<sup>81,82</sup>. Such applications eliminate draw solution regeneration and also highlight the promising aspects of FO for wastewater reuse.

Similar to *Figure 2.6-3*, a typical FO laboratory setup running on osmotic dilution mode includes a feed solution, suitable draw solution on a digital balance (for weight and ultimately, flux measurements), semi-permeable membrane in a cell, and flow pumps.



*Figure 2.6-4: FO laboratory setup*

The principle of FO operation relies on the osmotic pressure difference ( $\Delta\pi$ ) between the feed and draw solutions, among other factors. The osmotic pressure difference can be seen as the amount of hydrostatic pressure ( $\Delta P$ ), which if exerted on the draw solution will completely terminate the osmotic flow of water from the feed to the draw side<sup>83</sup>. The Van't Hoff equation can be employed for the calculation of the theoretical osmotic pressure for any solution:

$$\pi = RT \sum iM \quad (10)$$

where R is the gas constant in L.atm/mol. K, T is the solution temperature in Kelvin, i for a specific solution is the dimensionless Van't Hoff constant, and M is the molarity of the solution in mol/L. The resulting water flux ( $J_w$ ), from the osmotic pressure difference of the feed and draw solution, can also be computed as shown in Equation 11:

$$J_w = A_w(\Delta P - \Delta\pi) \quad (11)$$

where  $A_w$  is the water permeability coefficient (a membrane specific parameter).  $\Delta P$  is zero because there is no applied hydrostatic pressure in the forward osmosis process. Thus the above equation reduces to:

$$J_w = A_w(\pi_{draw} - \pi_{feed}) \quad (12)$$

Experimentally, the water flux can be computed as:

$$J_w = \frac{(V_{draw,f} - V_{draw,i})}{\Delta t \times A_{membrane}} \quad (13)$$

where  $V_{draw,f}$  and  $V_{draw,i}$  are the final and initial volumes of the draw solution,  $\Delta t$  is the time interval difference, and  $A_{membrane}$  is the effective surface area of the membrane.

In general, the performance of FO is mainly affected by the following factors – membrane characteristics and configuration; draw solution choice and concentration. Other factors include feed solution quality and operating conditions such as temperature and pH. In terms of membrane characteristics, optimization is essential for improved FO performance since water flux is also affected by membrane parameters such as tortuosity and thickness. Coday et al<sup>48</sup> describe the ideal FO membrane design to be a thin active and support layer whose pores have low tortuosity. Commercially available membranes include cellulose triacetate (CTA) and polyamide thin-film composite (TFC) membranes.

Several studies have focused on identifying effective draw solutions<sup>74,84</sup>. An ideal draw solute should be highly soluble in water and able to generate high osmotic pressure. Increased molar concentrations (M) of the draw solute can be achieved if draw solute readily dissociates in water, thus leading to higher osmotic pressure (Equation 10). Also, low molecular weight draw solutes, which are not highly viscous in water, are more desirable. This is mainly because the diffusivity (or diffusion coefficient) of the draw solute is inversely proportional to its molecular weight and viscosity<sup>74</sup>. Thus, if a draw solute has high molecular weight and viscosity, it will lead to a low diffusion coefficient, indicating that the draw solute has a low capacity to diffuse in and out of the support layer of membrane<sup>85</sup>. Low diffusion coefficient has however been reported to slightly contribute to internal concentration polarization (ICP), a major drawback of the FO process<sup>74,85</sup>. In the FO mode where the feed faces the active layer, dilutive ICP occurs when the draw solute in the support layer becomes more and more diluted from water permeation and ultimately reduces the osmotic pressure difference and water flux of the system. McCutcheon et al<sup>86</sup> report the equation that governs this mechanism:

$$J_w = \frac{1}{K} \ln \frac{A\pi_{draw} + B}{A\pi_{feed} + B + J_w} \quad (14)$$

$$K = \frac{t\tau}{D\varepsilon} \quad (15)$$

where  $t$ ,  $\tau$ ,  $\varepsilon$  and  $S$  are membrane-specific properties (namely, thickness, tortuosity, porosity, structural parameter).  $K$  is the resistance of the draw solution to support layer diffusion and  $D\varepsilon$  is the diffusion coefficient. It is evident that if a draw solute has a high diffusion coefficient,  $K$  will be lower. As a result, the draw solute can easily diffuse in and out of support layer and concentration polarization will be reduced. The authors conclude that in the FO mode, one feasible way to reduce ICP is to select a draw solute with higher diffusion coefficient. Lastly, an appropriate draw solute should have a low reverse salt flux (RSF). RSF is the reverse flow of the draw solute into the feed solution and it reduces the osmotic pressure difference (and thus water flux) of the system. Several draw solutes have been proposed for the FO process and downstream regeneration, toxicity and cost are other factors that were considered<sup>74,87</sup>. *Figure 2.3-5* shows different draw solutes and their corresponding osmotic pressures as a function of concentration.

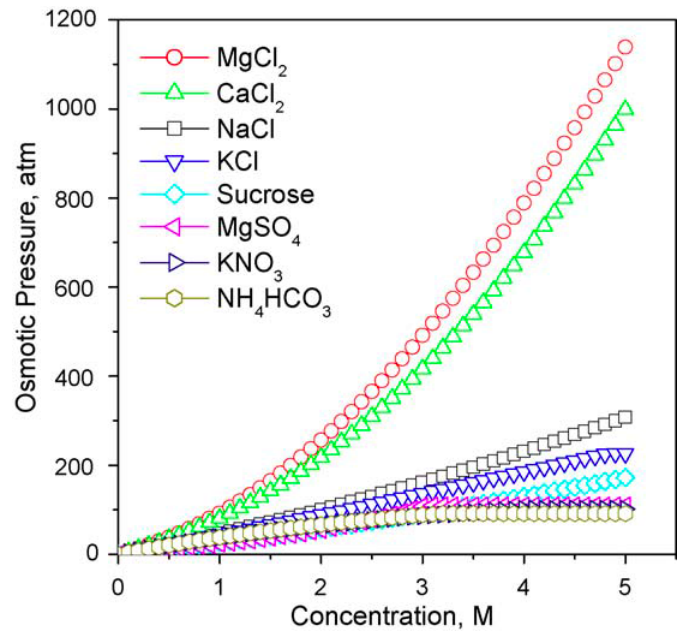


Figure 2.6-5: Osmotic pressure vs Concentration analysis for prospective draw solutes in the FO process<sup>88</sup>

## **Chapter 3 - Preliminary and Response Surface Methodology Experiments for Optimization of Parameters**

### **3.1 Introduction**

In this section, electrocoagulation parameters were studied in order to understand their effect on turbidity, COD and ion removal. There are several parameters that are known to affect pollutant removal efficiency in the electrocoagulation process such as pH, reaction time, current density, electrode distance, feed quality and electrode material<sup>89,90</sup>. Preliminary experiments were conducted and the following parameters were investigated in order to examine their effect on turbidity removal: electrode distance, pH, current density, time and electrode material. Synthetic wastewater was used, as supply of industrial wastewater was not yet confirmed. The ‘best’ set of EC conditions was determined (pH especially was chosen to accommodate the later addition of coagulant aid). Literature review showed that for the chosen coagulant aids, pH 5-7 is suitable for superior particle removal<sup>42</sup>.

Response Surface Methodology (RSM) was then applied to observe the interaction and significance of pH, current density and time on contaminant removal, specifically COD, calcium, iron and chloride removal. RSM is an advantageous statistical tool that overcomes the shortcomings of the one-factor-at-a-time method employed during the preliminary experiments. Through a reduced number of experiments, RSM can define the significance and interaction among factors in a multifactor experiment. Preliminary experiments are mainly helpful to narrow down the range to be observed in RSM for each factor. Industrial wastewater was used for experiments in this category primarily due to the more consistent water quality compared to synthetic wastewater.

Contour and surface plots were generated from RSM analysis based on suitable models, which were optimized for COD, calcium, iron and chloride removal. Industrial SGPW was then used to test the best preliminary experiment conditions and the optimum RSM conditions. Contaminant removals from both experiments were compared and conclusions on the efficiency of SGPW wastewater treatment via electrocoagulation were drawn.

## 3.2 Materials and Methods

### 3.2.1 Materials

For preliminary experiments, synthetic wastewater was prepared according to *Table 3.1*. Salt concentrations were determined based on literature review<sup>91,92</sup> and concentrations were adjusted for water content in hydrated salts. Chemicals were purchased from Sigma-Aldrich, USA and sand was filtered using a 75  $\mu\text{m}$  sieve.

Compound	Anhydrous salt concentration (g/L)	Adjusted hydrated concentration (g/L)
Sodium carbonate	0.66	
Sodium sulfate	0.74	
Sodium chloride	110.016	
Ferric chloride	0.16	
Barium chloride dihydrate	7.136	8.371
Magnesium chloride hexahydrate	7.917	16.905
Manganese chloride tetrahydrate	0.016	0.0252
Strontium chloride hexahydrate	12.286	20.66
Calcium bromide	2	
Calcium chloride	84.915	
Potassium chloride	1.182	
Sand	2.5	
Oil	0.7	

*Table 3.1: Synthetic wastewater composition for preliminary experiments.*

The laboratory electrocoagulation setup for both preliminary and RSM experiments is shown in *Figure 3.1*.

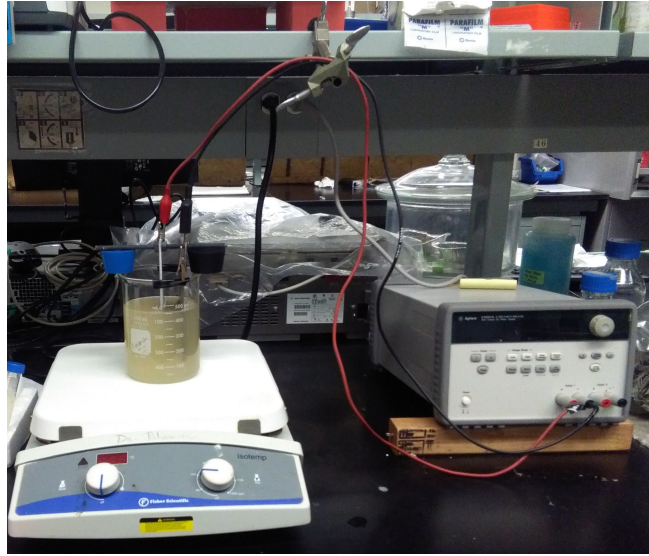


Figure 3.1: EC laboratory setup

For RSM experiments, SGPW was gotten from a company in Western Canada whose operations are in both Alberta and British Columbia. Wastewater analysis was performed by the company (Table 3.2a) and also at Concordia’s Environmental Engineering laboratory (Table 3.2b). Samples were stored at 4°C.

CATIONS				ANIONS			
Ion	mg/L	mmol/L	meq/L	Ion	mg/L	mmol/L	meq/L
Na <sup>+</sup>	54400.0	2366.3	2366.3	Cl <sup>-</sup>	109186.0	3079.8	3079.8
K <sup>+</sup>	1950.0	49.9	49.9	Br <sup>-</sup>	1850.0	23.2	23.2
Ca <sup>2+</sup>	8010.0	199.9	399.7	I <sup>-</sup>	29.6	0.2	0.2
Mg <sup>2+</sup>	909.0	37.4	74.8	HCO <sub>3</sub> <sup>-</sup>	174.5	2.9	2.9
Ba <sup>2+</sup>	501.0	3.6	7.3	SO <sub>4</sub> <sup>2-</sup>	50.3	0.5	1.0
Sr <sup>2+</sup>	1490.0	17.0	34.0	CO <sub>3</sub> <sup>2-</sup>	Nil	Nil	Nil
Fe <sup>2+</sup>	29.5	0.5	1.1	OH <sup>-</sup>	Nil	Nil	Nil
Total			2933.1	Total			3107.1

Table 3.2a – Produced water quality analysis (June 2015) from an unconventional oil and natural gas extraction field in Western Canada. Reported TDS = 174,591 mg/L and salinity = 17.64%

pH	5.40
Turbidity (NTU)	52.89
COD (mg/L)	15500
Fe (mg/L)	71.65
Ca (mg/L)	23193
Cl (mg/L)	110000

*Table 3.2b- Laboratory analysis of industrial wastewater for specific contaminants*

### **3.2.2 Methodology**

#### **3.2.2.1 Preliminary experiments**

Synthetic SGPW was prepared by first adding the specified oil concentration to about 700 ml of DI water and stirring at high speed for at least 12 hours. This was done in order to break oil droplets and form an oil-in-water emulsion. Salts were then added and DI water to raise the volume to one (1) liter. Sand was added to stimulate real SGPW and raise the TSS concentration. Wastewater was allowed to settle for 30 minutes and the supernatant was decanted.

450 ml of wastewater was poured into a 600 ml beaker and stirred at 100 rpm using a stir bar. pH was adjusted, if necessary, using 1M sulfuric acid and 1M sodium hydroxide solution. Electrodes were then placed into beaker and connected to the direct current (DC) power supply (Agilent Technologies) at a fixed current (0.18A-0.823A). Electrodes were either made of aluminum or iron (McMaster Carr) and an effective surface area of 0.0036 m<sup>2</sup> was immersed in the solution. Experiments were run for 60 min and time intervals for sample collection were 0 min (initial), 5min, 10, 20, 30, 40, 45, 60 min. At each time interval, about 10 ml was collected and voltage changes, pH and conductivity were recorded. The samples were then filtered with a 1.5 µm filter (GE) and turbidity was measured. Electrodes were washed using 300 ml washing solution (1M HCl), rinsed using tap and DI water, and dried prior to experiments.

### 3.2.2.2 Design of preliminary one-factor-at-a-time experiments

Experiments were performed first at different distance, then pH, current density and lastly, electrode material. Distance was varied from 1.1 to 3 cm (1.1, 2, 2.5, 3, 3.5 cm) for distance optimization experiments. 1.1 cm was the minimum distance achievable with electrodes. Anode/cathode combination used for distance, pH and current density experiments was Fe/Fe. Current density used for distance and pH experiments was 72.2 A/m<sup>2</sup> (0.259 A). There was no pH adjustment for distance experiments (Initial pH was around 7) and the distance that reported best turbidity removal was then employed for pH experiments.

pH 3,5,7,8,9 were investigated and the pH with the best turbidity removal over time was selected for current density experiments. 50, 100, 150, 200, 228.8 A/ m<sup>2</sup> were chosen for current density experiments. 228.8 A/ m<sup>2</sup> was the maximum attainable current density with the DC power supply used for experiments. After best turbidity removal was determined, the corresponding current density was applied for electrode material experiments. Al/Al, Al/Fe, Fe/Al and Fe/Fe were tested to determine the combination that maximizes turbidity reduction.

### 3.2.2.3 Response Surface Methodology Design of Experiments

Since industrial SGPW was used, no prior sample preparation was necessary. Minitab (Minitab, Inc.) was used to setup the design of experiments, which requires an input of low (-1) and high (+1) values of the variables (X<sub>i</sub>) examined. The following variables and ranges were applied:

Variables		Coded form of X <sub>i</sub>		
		-1	0	+1
Initial pH	X <sub>1</sub>	3	6	9
Reaction time (min)	X <sub>2</sub>	10	30	40
Current density (A/m <sup>2</sup> )	X <sub>3</sub>	45	130	215

Table 3.3a – Variables and their coded values for Central Composite Design

Center (0) values are calculated by taking the average of the low and high values and through a software-generated combination of the low, center and high values of each factor, the design of experiments was created as shown below:

RunOrder	pH (X <sub>1</sub> )	Time (X <sub>2</sub> )	Current Density (X <sub>3</sub> )
1	0	-1	0
2	-1	0	0
3	0	0	0
4	0	0	0
5	-1	1	1
6	0	0	-1
7	-1	1	-1
8	0	0	0
9	0	1	0
10	1	-1	1
11	0	0	1
12	1	-1	-1
13	-1	-1	-1
14	0	0	0
15	0	0	0
16	1	1	-1
17	-1	-1	1
18	1	1	1
19	0	0	0
20	1	0	0

*Table 3.3b – Design of Experiments for three variables: pH, current density and time*

A total of 20 experiments with different experimental conditions had to be performed. For each row in *Table 3.3b*, four response factors ( $Y_i$ ) – COD percent removal, iron percent removal, chloride percent removal and calcium percent removal - were measured. Percent removal was calculated by:

$$\% \text{ removal} = \frac{Y_0 - Y_i}{Y_0} \quad (16)$$

where  $Y_0$  and  $Y_i$  are the initial and final COD, iron, chloride or calcium concentration. These removal percentages were inputted into the software and regression analysis was performed to fit the data to an appropriate model. A quadratic model including three-way interactions (Equation 17) generated the best fit for the data based on the Analysis of Variance (ANOVA) report. The model included two-way and three-way interactions of the variables.

$$Y_i = \beta_0 + \sum_{i=1}^k \beta_i X_i + \sum_{i=1}^k \beta_{ii} X_i^2 + \sum_{i=1}^k \sum_{j=i+1}^k \beta_{ij} X_i X_j + \beta_{ijk} X_i X_j X_k + \varepsilon \quad (17)$$

where  $Y_i$  is the percent removal of the response factors  $X_i, X_j, X_k$  are the variables, and  $\beta_0, \beta_i, \beta_{ij}, \beta_{ii}, \beta_{ijk}$  are the regression coefficients for the intercept, linear, interaction, quadratic and cubic terms.

For each response factor, contour and main effects plots were generated to observe the effect of the interaction among variables. Contour plots were drawn around the center values. ANOVA reported the P-value (Probability value), which is a statistical value used to determine the significance of a variable. If the P-value for a variable is below 0.05, then the variable is significant for the removal of the contaminant. 0.05 is typically the default number for significance in most statistical analysis.

Although the main goal of performing the design of experiments was to determine significance of variables, the model was still optimized. Experiments were then conducted under optimum conditions and results were compared to those obtained when the best preliminary experiment conditions were applied to the same SGPW.

### 3.2.3 Analytical Methods

Turbidity readings were taken using a turbidity meter (HF Scientific) while pH was measured using a calibrated pH meter (Oakton Instruments, 310 series, Vernon Hills, IL USA). Prior to COD analysis, filtered samples were diluted using a 1:100 dilution factor and transferred to Hach COD (TNT 822) vials. COD concentrations were measured using a spectrophotometer (DR2800, Hach). TOC was measured using a TOC analyzer (Shimadzu Corporation, Japan). Samples were diluted 100 times and acidified using 1M HCl prior to analysis.

Conductivity was measured using a calibrated conductivity meter (Oakton Instruments, Vernon Hills, IL USA). Chloride reductions were measured using a chloride-specific probe (Cole-Parmer, Canada) connected to a dual pH-ion meter (Fisher Scientific). Samples were diluted 1000 times to accommodate the electrode's two-point calibration, which was performed prior to each chloride ion analysis. Calcium and iron concentrations were determined using an Atomic Absorption Spectrometer (PinAAcle 900F, PerkinElmer). 1000ppm standards (SCP Science) for each element were used to prepare different concentrations for calibration on the instrument. A 1:10 dilution factor was performed for iron analysis while a 1:1000 dilution was done for calcium analysis.

## 3.3 Results and Discussion

### 3.3.1 Preliminary experiments

The following conditions showed favorable turbidity removal over time (*Table 3.4*).

Variables	Turbidity removal(NTU)	Removal %
	0 min	40 min
Distance=2 cm	224.9	95.14
pH=7	176.4	99.55
Current density=200 A/m <sup>2</sup>	177.85	99.54
Anode-cathode=Al/Fe	175.45	97.685

*Table 3.4: Preliminary experimental results*

Forty (40) minutes electrolysis time showed satisfactory turbidity removal (95-99%) for each variable. Distance of 2 cm was chosen because a further increment in the electrode distance has been reported to increase electricity consumption<sup>63</sup>. *Figure 3.2* confirms that the farther the distance between electrodes, the higher the voltage requirement (and thus electrical energy) for EC

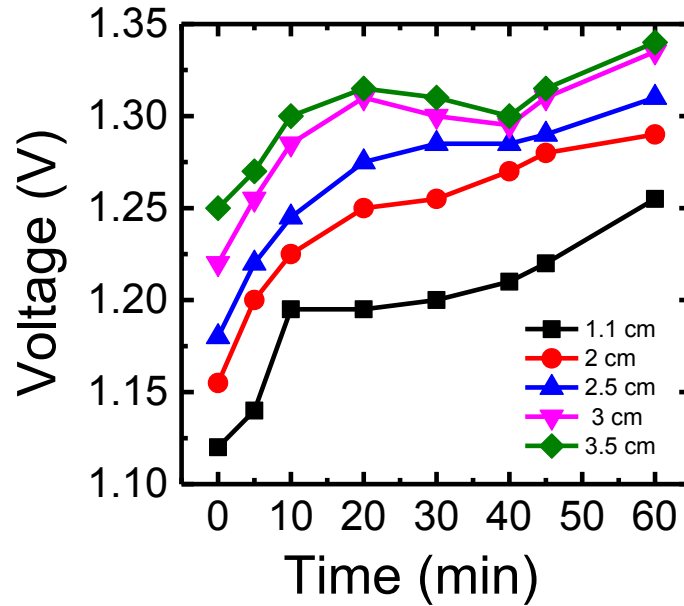


*Figure 3.2: Voltage increments over time for different electrode distances. Figure shows that as electrode distance increased, voltage increased over time*

Since the anode-cathode configuration used for pH experiments was Fe/Fe, pH 7 showed optimal turbidity removal most likely due to the insolubility of  $\text{Fe}^{3+}$  at neutral pH. More suspended and colloidal particles might have interacted with iron (iii) precipitates, which led to a higher turbidity removal<sup>93</sup>. In terms of current density, several researchers have shown experimentally that increasing current density affects contaminant removal and cost of the process since current density determines the rate of anode dissolution and thus, in-situ hydroxide formation<sup>53,90,94</sup>. *Figure 3.3* also confirms the incremental change in voltage as current density increases. Al/Fe was chosen in this work not only based on turbidity removal, but also based on literature review from similar studies.

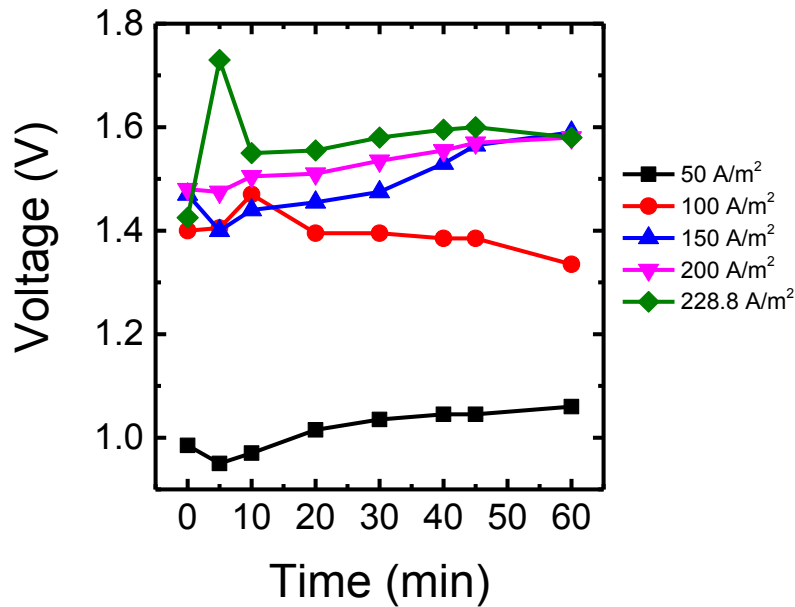


Figure 3.3: Voltage increments over time for different current densities. Figure shows that as current density increased, voltage increased over time

Gousmi, N. et al<sup>90</sup> conducted a study on the effect of electrode material on the treatment of petroleum refinery wastewater. They observed that Al/Al showed best turbidity and COD removal (99.94% and 83.52% respectively) followed by Al/Fe (99.24% and 81.51% respectively), Fe/Fe (98.45% and 78.57% respectively) and lastly, Fe/Al (98.30 % and 76.54% respectively). Researchers have attributed the higher removal efficiency for aluminum anodes to the formation of insoluble aluminum hydroxide flocs over a wider pH range (4-8)<sup>60</sup>. On the other hand, iron anodes form insoluble iron hydroxide flocs, which are mainly effective around neutral and alkaline pH. At this pH, the ratio of insoluble Fe<sup>3+</sup> to soluble Fe<sup>2+</sup> is higher.

Cathode passivation was also observed during preliminary experiments and as mentioned in *Section 2.6.1*, the presence of chloride ions assisted in breaking the oxide film that formed on the cathode surface. *Figure 3.4* shows the cathode surface at 60 minutes for one of the distance experiments and as expected, part of the film was broken. pH measurements also showed a sharp pH decrease and its steadiness around pH 5-6 during the distance and current density experiments (*Figure 3.5*). This might have

strengthened the stability and effectiveness of the active chlorine species against cathode passivation.

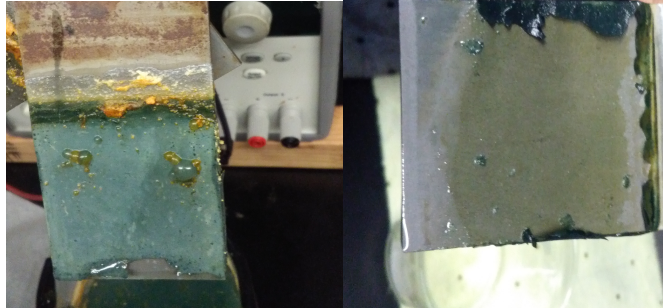


Figure 3.4: Cathode passivation on Fe electrode after 60 min

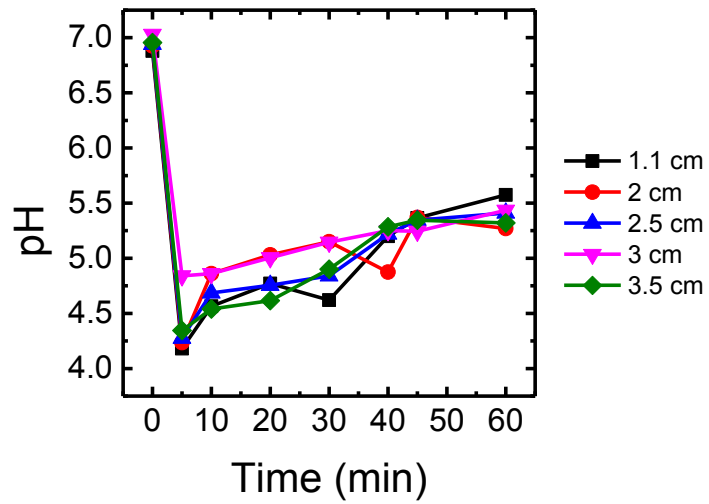


Figure 3.5: pH trend for different electrode distances.

Based on preliminary experiments, Al/Fe combination and 2 cm distance was used for RSM experiments. pH, current density and time were varied to observe the significance and interaction among parameters and their effect on COD, calcium, iron and chloride removal.

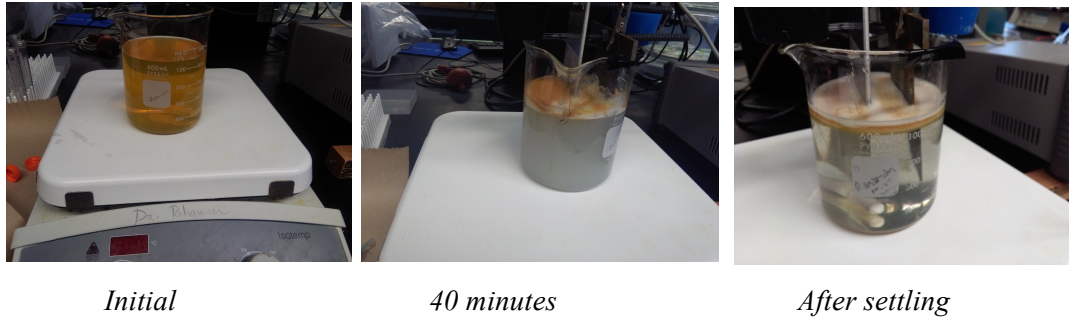
### 3.3.2 RSM experiments

Table 3.5 summarizes the experimental and predicted responses obtained for COD, iron, calcium and chloride removals using industrial SGPW.

Run Order	% COD removal (Y <sub>1</sub> )		% Cl- removal (Y <sub>2</sub> )		% Ca removal (Y <sub>3</sub> )		% Fe removal (Y <sub>4</sub> )	
	Exp.	Pred.	Exp.	Pred.	Exp.	Pred.	Exp.	Pred.
1	28.42	23.60	23.88	29.38	16.32	16.21	72.46	76.68
2	44.95	42.70	29.12	29.96	18.80	18.69	67.18	67.83
3	19.18	32.66	23.48	27.34	20.34	15.56	71.61	79.67
4	23.11	32.66	26.82	27.34	11.65	15.56	77.56	79.67
5	47.58	47.76	18.89	20.30	14.00	14.03	61.37	62.70
6	37.68	32.87	18.76	24.46	25.25	25.14	83.18	85.50
7	33.33	33.89	35.32	35.06	19.37	19.40	78.83	79.14
8	36.36	32.66	23.77	27.34	14.81	15.56	81.71	79.67
9	39.89	36.60	27.7	26.94	13.53	13.42	82.80	79.14
10	20.95	22.42	29.91	28.98	14.73	14.76	80.57	80.12
11	33.48	30.19	22.94	21.98	14.55	14.44	82.57	80.82
12	21.91	23.75	29.31	26.72	22.05	22.07	79.01	77.54
13	40.87	41.81	31.53	29.71	16.86	16.89	73.14	71.48
14	43.07	32.66	33.79	27.34	15.95	15.56	83.64	79.67
15	24.07	32.66	32.76	27.34	14.86	15.56	82.62	79.67
16	50.97	52.43	16.57	15.54	17.26	17.28	79.70	80.20
17	31.97	32.54	21.69	21.53	19.85	19.88	65.58	64.94
18	37.36	38.44	25.66	26.30	23.94	23.97	80.36	81.88
19	33.98	32.66	32.93	27.34	15.31	15.56	82.00	79.67
20	43.81	37.96	23.79	27.69	11.51	11.40	78.29	78.20

Table 3.5 – Design of twenty (20) experiments: variables and the corresponding experimental and predicted responses

Turbidity removal ranged from 97.88 – 100% for all experiments. *Figure 3.6* shows the physical changes of the wastewater sample during the electrolysis time.



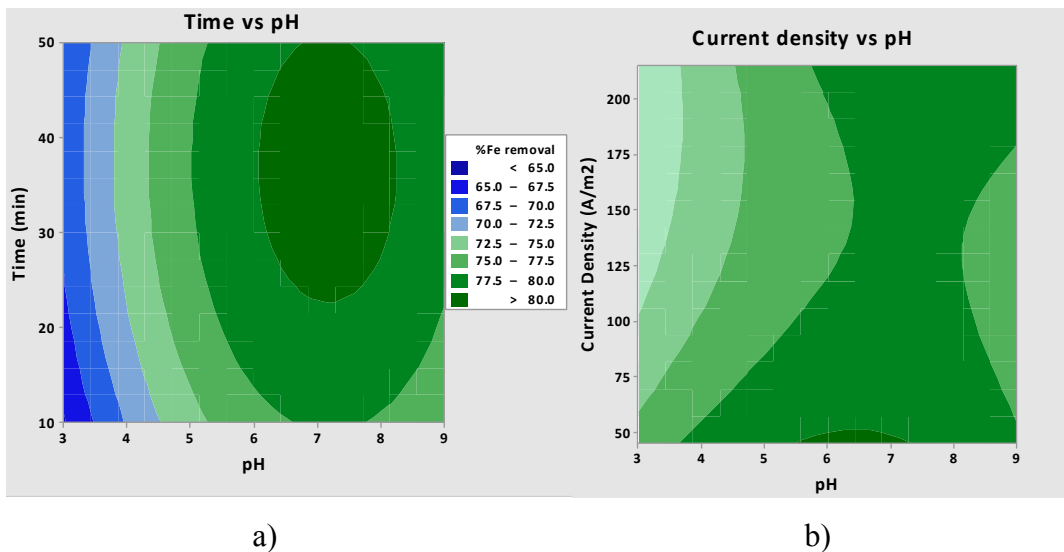
*Figure 3.6: Color changes of SGPW during EC*

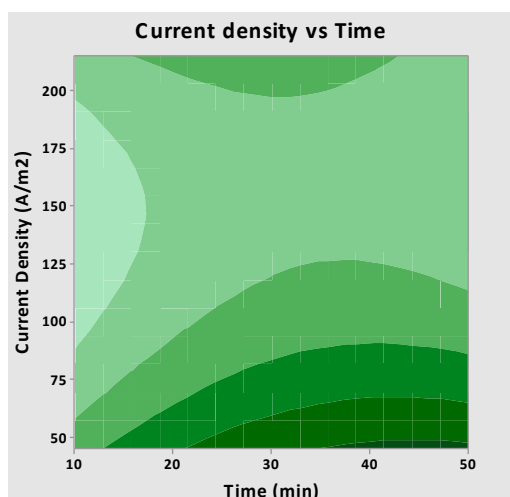
### Iron removal

The regression equation for iron removal is described in Equation 18 ( $R^2 = 80.84\%$ ):

$$Y_4 = 50.4 + 9.78X_1 + 0.613X_2 - 0.170X_3 - 0.739X_1^2 - 0.00439X_2^2 + 0.000483X_3^2 - 0.0308X_1X_2 + 0.0067X_1X_3 - 0.002124X_2X_3 + 0.000221X_1X_2X_3 \quad (18)$$

*Figure 14a* illustrates the effect of pH, time and current density on iron removal. For each contour plot, the y-axis label for the first plot is time while the x-axis label is pH. The second on the right is a plot of current density (y-axis) and pH (x-axis). Lastly, the third is a plot of current density (y-axis) vs time (x-axis).





c)

Figure 3.7: %Fe removal contour plots describing interactions between a) time and pH, b) current density and pH, and c) current density and time

Maximum iron removal was observed around pH 6.5-8, current density  $< 50 \text{ A/m}^2$  and time = 30-50 minutes. pH greater than 6.5 has been reported to be effective for the precipitation of Fe in the presence of oxygen<sup>93</sup> because at pH 7,  $\text{Fe}^{2+}$  is oxidized to insoluble  $\text{Fe}^{3+}$ . When the solution pH becomes acidic, the oxidation of ferrous iron ( $\text{Fe}^{2+}$ ) to ferric iron ( $\text{Fe}^{3+}$ ) diminishes and therefore the metal removal decreases<sup>89</sup>. Neutral and alkaline pH, however, tends to favor oxidation of  $\text{Fe}^{2+}$  to  $\text{Fe}^{3+}$  as well as their complex polymerization, which aids organics (and COD) removal. In addition, some compounds might react with soluble  $\text{Fe}^{2+}$  to form precipitates, which leads to more iron removal<sup>89</sup>. ANOVA also confirmed the significance of pH for the removal of iron. P-value for both linear and quadratic pH terms were 0.026, which is less than 0.05.

Figure 3.8 also shows the main effects plot for iron removal. It describes the average change in the response factor as the values of the variable change from low to high. The vertical axis is the mean removal of each response factor and the horizontal axis is the low, center and high values for each variable. From Figure 3.8, increasing both pH and time from low to center values results in higher removal of iron. However, further increases of both pH and time result in a negative slope, which point to a decrease in iron

removal. Current density plot is also downward sloping, which means that increasing the current density reduces iron removal, but only by 3% (on average).

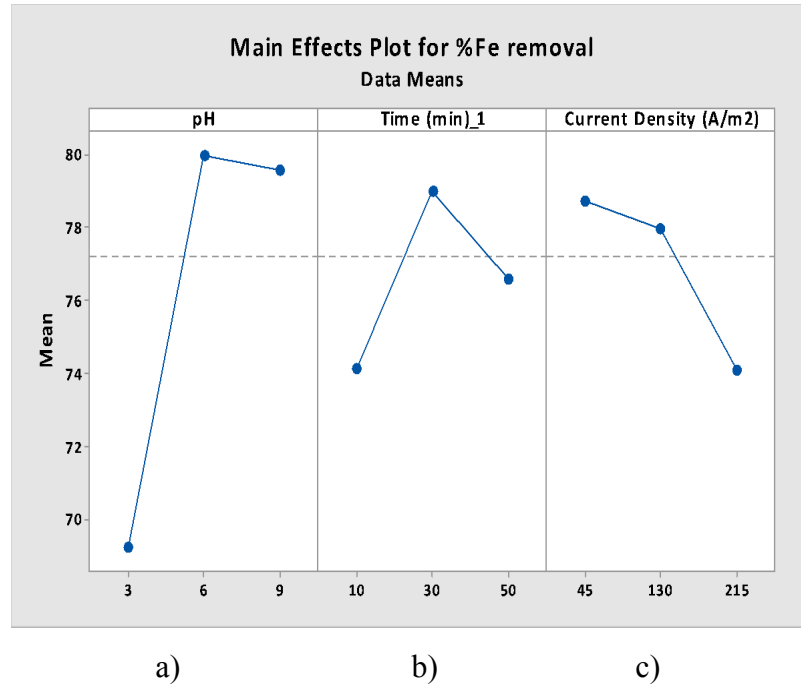


Figure 3.8: Main effects plot for iron removal showing mean removal for a) incremental pH changes, b) incremental time, and c) incremental current densities.

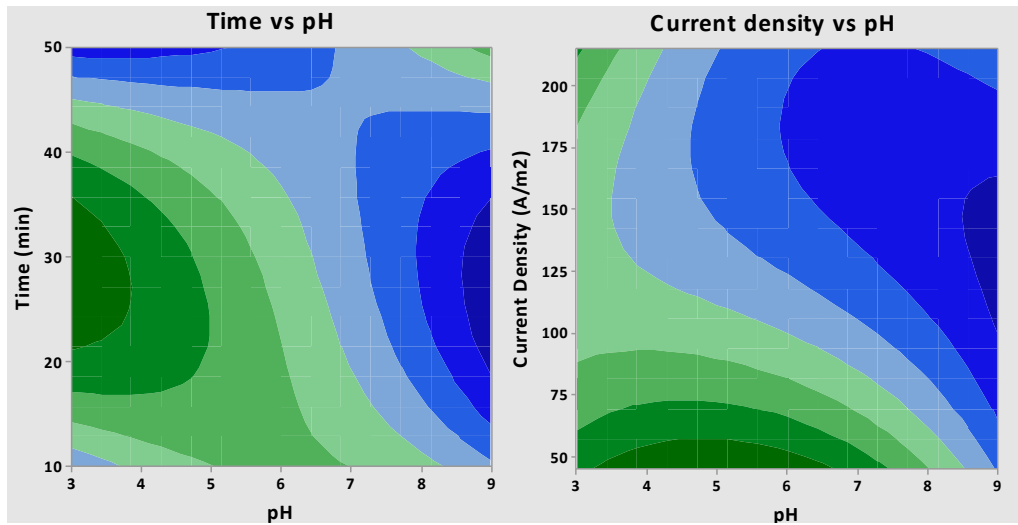
The model was also asked to predict iron removal if the best preliminary experimental conditions (pH 7, time = 40 minutes and current density = 200 A/m<sup>2</sup>) were applied. A removal of 81.78% was predicted and after conducting experiments under the same conditions using industrial SGPW, 75.56% removal was observed.

### Calcium removal

The regression equation for calcium removal is described in Equation 19 ( $R^2 = 85.64\%$ ):

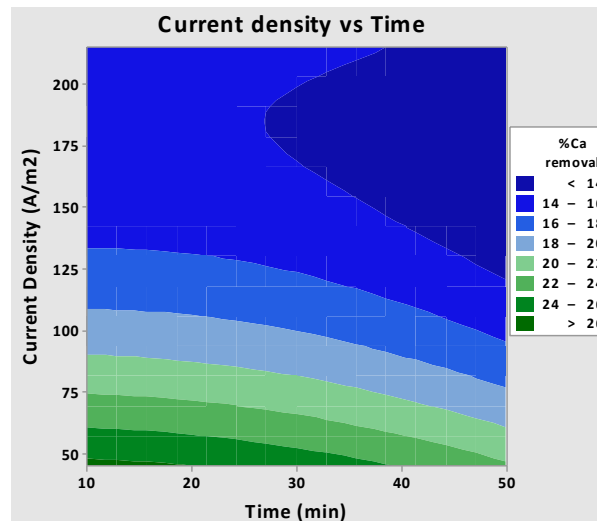
$$\begin{aligned}
 Y_3 = & -28.8 + 17.69X_1 + 2.014X_2 + 0.1X_3 - 1.157X_1^2 - 0.025X_2^2 + 0.000586X_3^2 - \\
 & 0.389X_1X_2 - 0.0936X_1X_3 - 0.00288X_2X_3 + 0.0085X_1X_1X_2 + 0.0065X_1X_1X_3 + \\
 & 0.00386X_1X_2X_2 + 0.000548X_1X_2X_3
 \end{aligned} \tag{19}$$

Figure 3.9 shows the effects of pH, time and current density on calcium removal.



a)

b)



c)

Figure 3.9: %Ca removal contour plot describing interactions between a) time and pH, b) current density and pH, and c) current density and time

Maximum calcium removal for this wastewater was around acidic-neutral pH, time around 30-35 min and CD  $< 55 \text{ A/m}^2$ . According to ANOVA, the linear terms of pH (P-value = 0.031), time (P-value = 0.036) and the cubic interaction of pH, time and current density (P-value = 0.022) were significant for calcium removal. The quadratic effect of current density, and the quadratic interaction of pH and current density were also significant (P-values were 0.034 and 0.028 respectively).

The dependence of calcium removal on current density has also been studied. Oncel et al<sup>96</sup> compared the ability of chemical precipitation and electrocoagulation processes to remove metals in coal acid drainage wastewater. The chemical precipitation process did not lead to any significant reduction in calcium concentration, until pH 10 was reached, due to the high solubility and amphoteric nature of calcium hydroxide. Initial calcium concentration was 259.6 mg/L and at pH 10, concentration reduced to 172.60 mg/L (33.5% reduction). A significant amount of sodium hydroxide was however needed to raise the pH to 10, which renders the treatment cost inefficient. The electrocoagulation study was conducted at the normal pH of the wastewater (2.5) and for 40 minutes. Four iron electrodes were used alternately as anode and cathode to treat 1 L of wastewater. The authors observed that increasing the current density from 200 to 400 A/m<sup>2</sup> did not show a remarkable removal of calcium. However, when the current density was raised to 500 A/m<sup>2</sup> (18 A), calcium concentration dropped dramatically, from an initial concentration of 259.6 mg/L to 0.104 mg/L at 500 A/m<sup>2</sup>. The authors explained that high current density enables the formation of more metal hydroxide complexes, which greatly improves metal removal. It is obvious that the cost, energy consumption and sludge generation from applying such a large current density will be enormous. The authors calculated an operating cost of 1.98 €/m<sup>3</sup>, energy consumption of 5.64 kWh/m<sup>3</sup> and 3.58 kg/m<sup>3</sup> sludge generation at 500 A/m<sup>2</sup> compared to a cost of 0.91 €/m<sup>3</sup>, energy consumption of 1.32 kWh/m<sup>3</sup> and 0.85 kg/m<sup>3</sup> sludge produced at 200 A/m<sup>2</sup>. This study thus highlights the challenge in removing a high percentage of calcium from SGPW.

The regression equation predicted a removal of 13.69% for the best preliminary experimental conditions. A removal of 13.66% was observed experimentally. *Figure 3.10* describes the main effects plot for calcium removal. Similar to the contour plots, lower current density and acidic pH are suitable for better calcium removal from this SGPW.

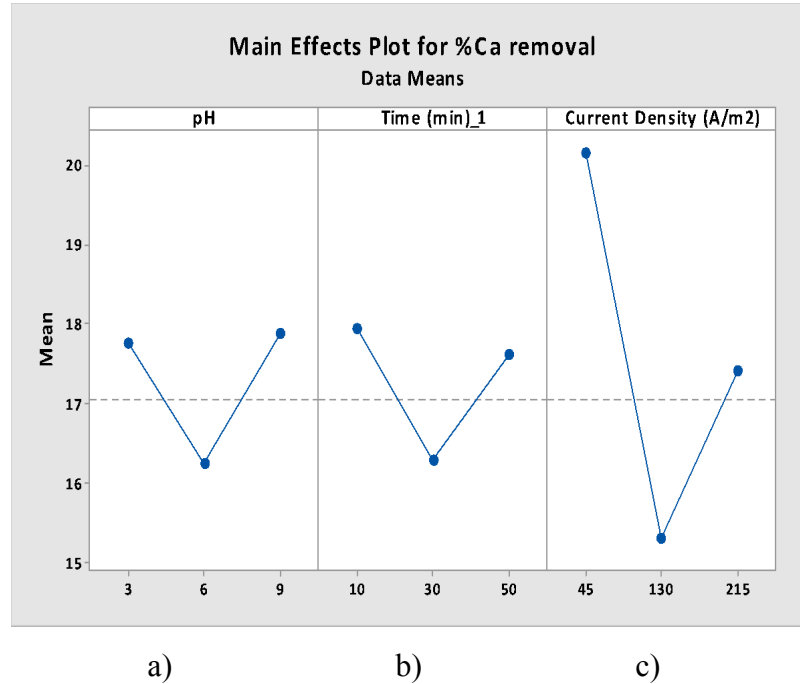


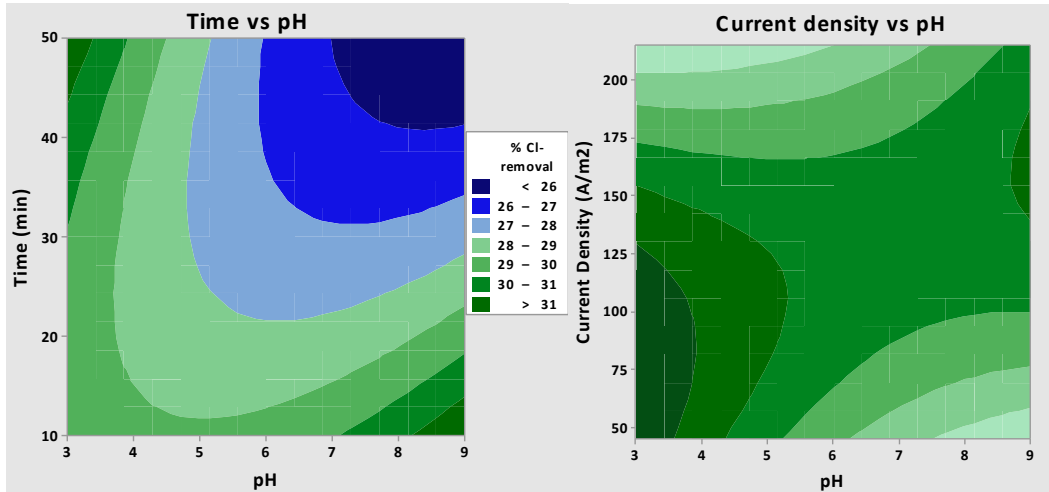
Figure 3.10: Main effects plot for iron removal showing mean removal for a) incremental pH changes, b) incremental time, and c) incremental current densities.

### Chloride (Cl) removal

The regression equation for chloride ion removal is described in Equation 20 ( $R^2 = 59.03\%$ ):

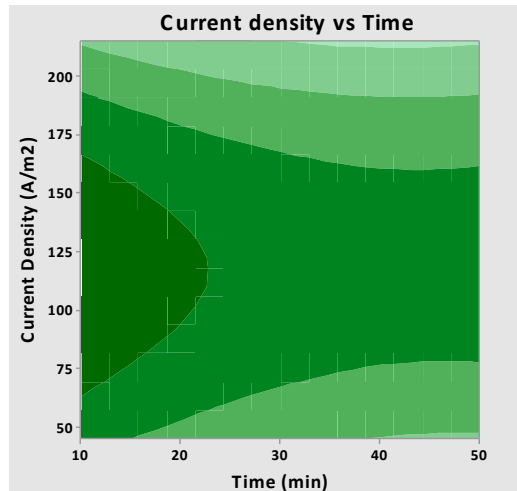
$$Y_2 = 30.3 - 2.08X_1 + 0.312X_2 + 0.09X_3 + 0.165X_1^2 + 0.00204X_2^2 - 0.000571X_3^2 - 0.0855X_1X_2 + 0.0065X_1X_3 - 0.00208X_2X_3 + 0.00037X_1X_2X_3 \quad (20)$$

The above regression model for chloride removal was the best that generated the highest  $R^2$  value. Figure 3.11 describes the effects of pH, time and current density on chloride removal.



a)

b)



c)

Figure 3.11: %Cl<sup>-</sup> removal contour plot describing interactions between a) time and pH, b) current density and pH, and c) current density and time

ANOVA reported that no variables were significant for chloride ion removal. Xia et al<sup>97</sup> claimed that chloride removal up to 34% is achievable only under certain conditions: “adding a magnesium compound whose ion weight concentration is less than about 20% of the initial chloride ion concentration; adding at least two compounds containing calcium, aluminate and hydroxide ions and lastly, a pH > 10 after adding at least two of the compounds”. These specific conditions increase the complexity of the reduction of chloride concentration in SGPW. Nevertheless, under the best preliminary experimental conditions, the model predicted a removal of 24.12%, with a 95% confidence interval

range of 18.1% - 30.15%. We observed a close value of 20.94% experimentally. *Figure 3.12* is the main effects plot for chloride removal. The average reduction in chloride removal for an increment from low to high values for each variable varied from 2-4%.

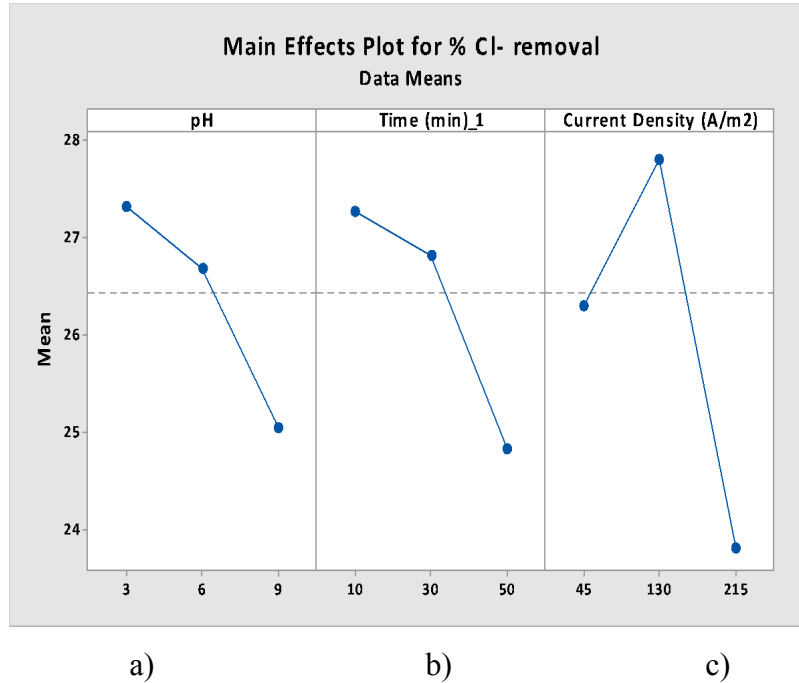


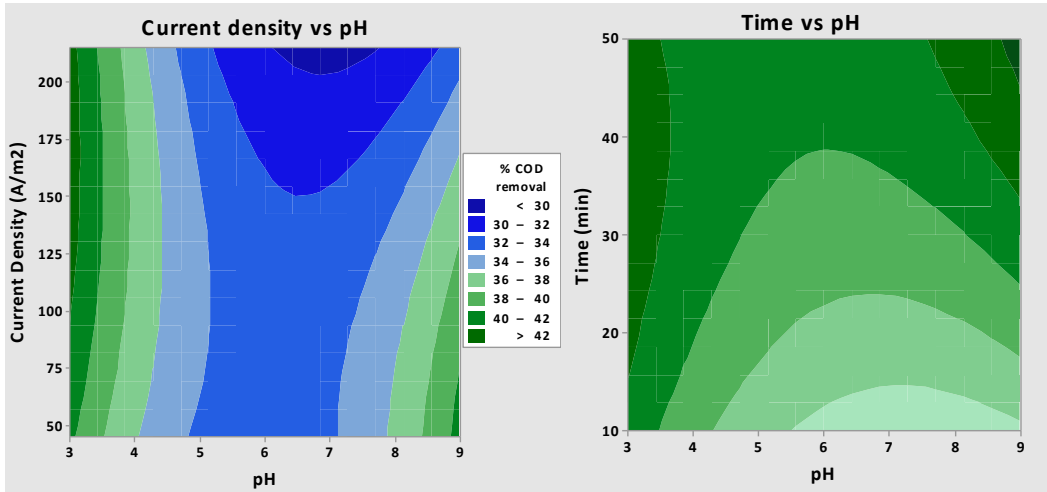
*Figure 3.12: %Cl<sup>-</sup> removal contour plot describing mean removal for a) incremental pH changes, b) incremental time, and c) incremental current densities.*

### COD removal

The regression equation for COD removal is described in Equation 21 below ( $R^2 = 64.64\%$ ):

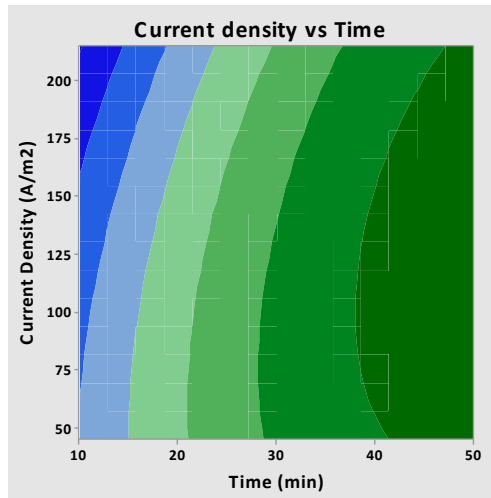
$$Y_1 = 81.9 - 15.5X_1 - 0.543X_2 - 0.097X_3 + 0.852X_1^2 - 0.0064X_2^2 - 0.000157X_3^2 + 0.1920X_1X_2 + 0.0166X_1X_3 + 0.00604X_2X_3 - 0.000877X_1X_2X_3 \quad (21)$$

*Figure 3.13* illustrates the effect of pH, time and current density on COD removal. Maximum COD removal was observed around acidic or very alkaline pH, time greater than about 35 minutes and a wide current density range. ANOVA showed that the pH term and the quadratic interaction between pH and time were slightly significant (P values were 0.06 and 0.055 respectively).



a)

b)



c)

Figure 3.13: %COD removal contour plot describing interactions between a) time and pH, b) current density and pH, and c) current density and time

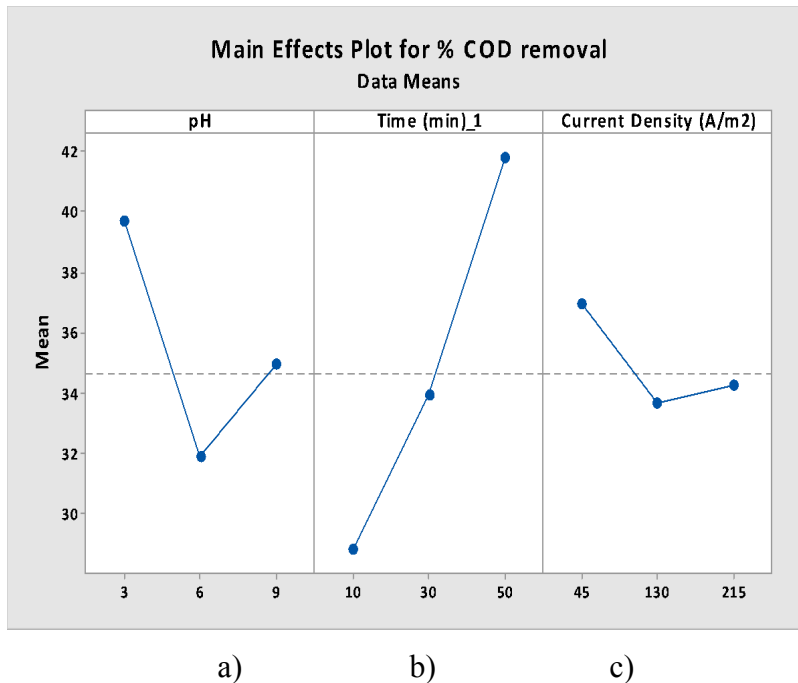


Figure 3.14: %COD removal main effects plot describing mean removal for a) incremental pH changes, b) incremental time, and c) incremental current densities.

Initial COD is about 15000 mg/L and under the best preliminary experiment conditions, model predicted 33.4815% COD removal with 95% confidence interval (range: 23.73% - 43.21%). From experiments, COD removal was calculated as 26.37%. More explanation on possible COD removal mechanisms will be discussed in the following subsection.

#### Optimized conditions

The *Response Optimizer* option on Minitab allows for optimization in order to attain the best removal of contaminants. Regression models were optimized and the following conditions were determined to give the best removal for COD, calcium, iron and chloride:

$$\text{pH} = 3.2, \text{Time} = 35 \text{ minutes and current density} = 45 \text{ A/m}^2$$

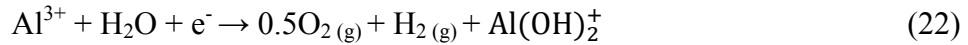
Electrocoagulation experiments were performed under the above conditions and COD and ion removals were compared with those from preliminary experiment conditions. Results are presented in *Table 3.6*.

	pH = 7, Time = 40 min, CD = 200 A/m <sup>2</sup>	pH = 3.2, Time = 35 min, CD = 45 A/m <sup>2</sup>
COD	26.37	47.27
Fe	75.56	60.76
Cl	20.94	24.925
Ca	13.66	12.96

Table 3.6: COD and ion removals under preliminary and optimized conditions

Higher COD removal was observed under acidic conditions compared to the neutral pH condition in preliminary experiments. This is also evident from the COD contour and main effects plots (*Figure 3.13* and *3.14*). A discussion on the speciation of aluminum under different pH conditions is necessary in order to explain possible COD removal mechanisms.

Aluminum speciation, in the form of monomeric, polymeric species and precipitates, is dependent on pH and aluminum concentration in the solution. Monomeric species include  $Al^{3+}$ ,  $Al(OH)^{2+}$ ,  $Al(OH)_2^+$ , and  $Al(OH)_3$  while polymeric species could consist mainly of  $Al_{13}O_4(OH)_2^{6+}$ <sup>98,99</sup>.  $Al(OH)_3$  precipitates form predominantly at neutral pH. When pH is in the acidic range and aluminum dosage is low, monomeric hydroxoaluminum cations become prevalent while at high aluminum dosages, monomeric, polymeric and precipitate species form, according to the following possible reaction mechanisms<sup>99-101</sup>:



It is reasonable to say that the aluminum dosage is relatively low in the acidic condition (45 A/m<sup>2</sup>) compared to preliminary experiment condition (200 A/m<sup>2</sup>). As a result, it can be assumed that mainly monomeric hydroxoaluminum species are present. For the organic portion of COD, the generation of oxygen, according to Equation 22 might have helped in its removal. The presence of dissolved  $Fe^{2+}$  might have also assisted in organics removal, as the reaction between  $Fe^{2+}$  and acids like citric and salicylic acid has been reported to form insoluble products<sup>14</sup>. In addition, complex reactions and/or sorption between organics and hydrolyzed aluminum species could have aided in organics reduction.

For the inorganic portion of COD, main removal mechanisms are most likely through charge neutralization with positively charged monomeric flocs and/or interaction with hydroxyl groups and other cations generated from the reactions at the anode, cathode, and in the solution. These mechanisms might have been more pronounced for the removal of other ions than calcium and iron since both showed lower removal in acidic pH compared to neutral pH conditions. Chloride removal was however slightly higher in the acidic pH condition. Sarpola<sup>98</sup> explored the influence of several parameters including presence of chloride and sulphate on aluminum hydrolysis. The author reported that there is indeed competition among anions for hydrolyzed aluminum in a solution. In a solution with chloride and sulphate, chloride, due to its relatively inert nature, does not form strong bonds with complexes of hydrolyzed aluminum species. It could attach to the terminal ends of the hydrolyzed species whereas sulfate binds strongly and could even act as a bridge between unhydrolyzed Al atoms. The ratio of the concentration of sulfate to chloride for the wastewater samples is however relatively low due to the high concentration of chloride.

As a result, the formation of both positively charged monomeric and precipitate species in the acidic condition might have provided a favorable environment for interaction and removal of more chloride than in the neutral condition, where mainly aluminum hydroxide precipitates form. For iron, reduced removal was observed since  $Fe^{2+}$  is soluble in acidic pH, as discussed in the *Iron Removal* subsection. For calcium, as discussed in the *Calcium Removal* subsection, the relatively higher current density in the neutral condition might have led to the slightly better removal since calcium hydroxide precipitates are amphoteric and very high current densities up to  $500 \text{ A/m}^2$  were required for significant removal in one study<sup>96</sup>.

### 3.3.3 Energy and Electrode consumption

Electrode and energy consumption can be calculated according to Equations 25 and 26<sup>96</sup>:

$$\text{Electrode consumption } \left(\frac{kg}{m^3}\right) = \frac{M_w It}{FzV} \quad (25)$$

Where  $M_w$  is the molecular weight of the anode material ( $Al = 26.981 \text{ g/mol}$ ),  $I$  is the applied current in Amperes (A),  $t$  is the reaction time in minutes,  $F$  is Faraday's constant

(96,487 C/mol),  $z$  is the valence of the anode material ( $z_{Al} = 3$ ) and  $V$  is the volume of the wastewater in  $m^3$

$$\text{Energy consumption } \left(\frac{kWh}{m^3}\right) = \frac{UIt}{V} \quad (26)$$

Where  $U$  is the average voltage,  $I$  is the applied current in Amperes (A),  $t$  is the reaction time in hours, and  $V$  is the volume of the wastewater in  $m^3$ . Energy cost for treating 1  $m^3$  of SGPW was calculated by multiplying energy consumption by the energy charge of \$0.0550 per kWh (BC Hydro, Large General Service rate).

### ***3.3.3.1 Best preliminary experimental conditions***

The high conductivity of the synthetic wastewater reduced the current and voltage demand for the treatment process. Since constant current was applied (0.72 A), voltage varied from 1.155 V to 1.89 V (average at 40 minutes = 1.37 V). Thus, the calculated energy and electrode consumption, based on equations 25 and 26, were 1461.33 kWh/ $m^3$  and 5.97 kg/ $m^3$  (5970 mg/L) respectively. Energy cost was calculated as 80.37 CAD per  $m^3$  of SGPW.

### ***3.3.3.2 Optimized RSM conditions***

SGPW received from industry was also highly conductive. As a result, voltage as low as 0.54V was observed for constant current of 0.162 A (average at 35 minutes = 0.89 V). Despite the initially acidic condition, the pH increased as expected due to the buffering capacity of the process. The calculated energy and electrode consumption were 113.40 kWh/ $m^3$  and 1.17 kg/ $m^3$  (1170 mg/L) respectively. Energy cost was calculated as 6.237 CAD per  $m^3$  of SGPW.

## **3.4 Conclusions**

Preliminary one-factor-at-a-time experiments using synthetic wastewater were performed to establish distance, type of electrode material, pH, time and current density for electrocoagulation. Results showed satisfactory turbidity removal at distance = 2 cm, electrode material = Al/Fe, pH = 7, time = 40 minutes and current density = 200 A/ $m^2$ . The same distance and electrode material were used for response surface methodology experiments, which were done to observe the interaction and effect of pH, time and

current density on COD, calcium, iron and chloride removal. Design of experiments generated twenty (20) experiments which were performed and results were fit to a regression model. Analysis of Variance reported satisfactory  $R^2$  values and the significance of each EC parameter on pollutant removal.

For iron removal, similar to literature, pH was found to be significant. pH, time and current density were significant for calcium removal while for COD removal, pH and time were slightly significant. However, chloride removal was independent of any of the studied electrocoagulation parameters. Models for COD, calcium, chloride and iron removals were optimized and the optimum conditions were pH = 3.2, time = 35 minutes and current density = 45 A/m<sup>2</sup>. Under these conditions, COD removal up to 47.27% was attained compared to 26% removal when the best preliminary experiment conditions were applied for the same wastewater. Nevertheless, relatively lower ion removals (except for chloride) were observed under the optimized RSM conditions.

Acidic pH might have been favorable for the removal of organics and ions other than calcium and iron due to oxygen generation during anodic dissolution, complex reactions and/or sorption to hydroxoaluminum monomers in this acidic environment. Chloride ion showed better removal under acidic pH due to the generation of both positively charged monomeric species and precipitate species whose surface charge is also positive. Solubility of iron in acidic condition and nature of hydrolyzed calcium precipitate might have contributed to the observed, lesser removal under acidic pH. Electrocoagulation proved to be a very cost effective solution for treating SGPW since it takes advantage of the highly conductive nature of the wastewater. Optimized RSM condition reported lower energy and electrode consumption compared to preliminary experiment conditions.

There is a trade-off in deciding which condition is better for SGPW treatment. Optimum RSM condition (pH 3.2, time = 35 minutes and current density = 45 A/m<sup>2</sup>) is more cost-effective, reduces chloride (about 25%) and COD significantly. Nevertheless, preliminary experiment condition showed better removal of calcium and iron.

## Chapter 4 – Effect of Coagulant Aid Addition on COD and Ion Removal in Hydraulic Fracturing Wastewater

### 4.1 Introduction

Coagulant aids have been applied for wastewater treatment<sup>38-42</sup> and they are known to impact flocculation and thus treatment efficiency<sup>15</sup>. Coagulant aids could be anionic, cationic or nonionic polyelectrolytes. The goal of this chapter is to investigate the hypothesis that the addition of coagulant aid will further improve the extent of contaminant removal in the electrocoagulation process. To achieve this, two polymers, anionic and nonionic, were selected based on literature review and a study on the influence of polymer charge on pollutant removal was also conducted. COD and iron removal were examined for experiments using the nonionic polymer. COD, calcium, chloride, and iron reductions were observed for the anionic polymer. A discussion on possible contaminant removal mechanisms for each polymer is also provided.

### 4.2 Materials and Methods

#### 4.2.1 Materials

Polyacrylic acid (PAA) (average molecular weight = 1800) and nonionic polyacrylamide (nPAM) (average molecular weight = 5,000,000-6,000,000) were selected as the anionic and nonionic polymers, respectively. Their molecular structures are described below:

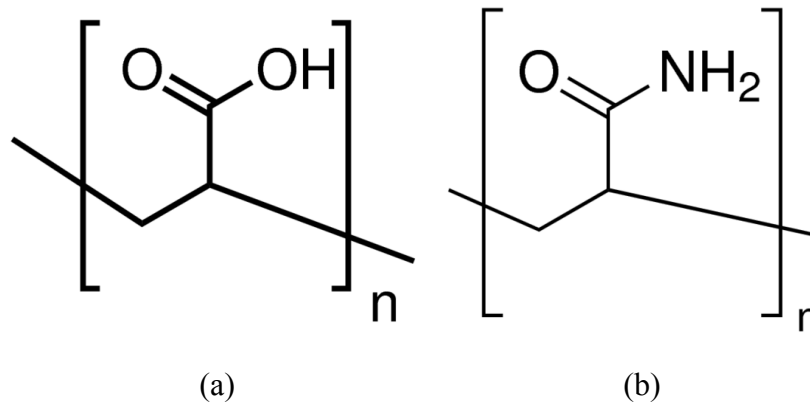


Figure 4.1: Molecular structure of a) polyacrylic acid and b) nonionic polyacrylamide (Sigma-Aldrich)

Both chemicals were purchased from Sigma-Aldrich. A new batch of wastewater samples (Batch 2) was received from the same company for experiments with PAA. The samples were less orange in color compared to the previous batch (Batch 1) (*Figure 4.2*). Average initial calcium, iron and chloride concentrations for Batch 2 samples were 19,692 mg/L, 19.24 mg/L and 86,400 mg/L respectively. pH and initial COD were 5.40 and 14900 mg/L.



*Figure 4.2: New SGPW (left) and old SGPW (right)*

#### **4.2.2 Methodology**

Batch 1 samples were used for experiments with nPAM and the remnant was also used for neutral pH-PAA experiments in order to compare results with Batch 2 samples, which were employed for the remainder of the experiments in this thesis. 450 ml of industrial SGPW was measured into a 600 ml beaker. 25 ppm of PAA or 20 ppm of nPAM was added to the EC beaker and stirred at 350 rpm for five (5) minutes. These coagulant aid concentrations were taken directly from literature<sup>42</sup>. pH was adjusted using 1M hydrochloric acid or 1M sodium hydroxide and initial samples were collected. Stirring was then reduced to 100 rpm and electrodes were placed in beaker and connected to the DC power supply. The current applied depended on whether preliminary or optimized RSM conditions were investigated. Final samples were taken at the end of the experiments and analyzed for COD, calcium, chloride and iron removal.

### 4.3 Results and Discussion

#### 4.3.1 Nonionic Polyacrylamide (nPAM)

When nPAM was applied as coagulant aid under preliminary experiment conditions (pH 7, current density = 200 A/m<sup>2</sup>, time = 40 minutes), the percent COD removal was 4% less than the case with no coagulant aid (*Figure 4.3*).

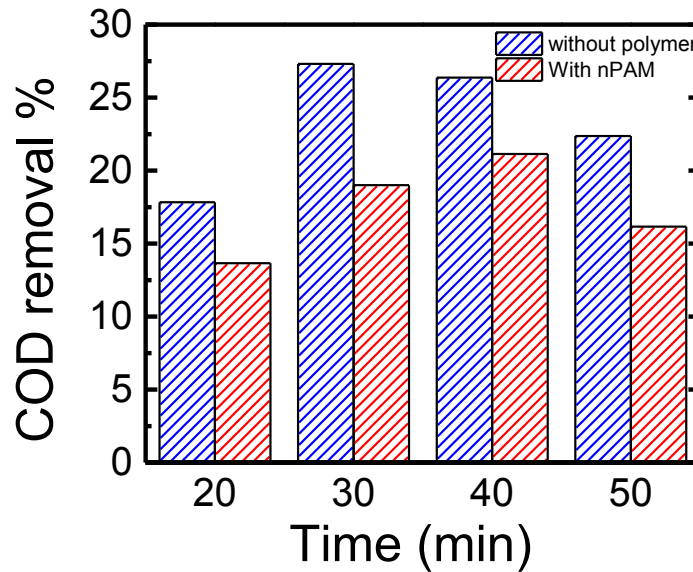


*Figure 4.3: % COD removal over time with and without nPAM*

Iron removals for both scenarios were similar - 76.25% (with nPAM) and 75.56% (no nPAM). The main mechanism of contaminant removal for such a polymer is interparticle bridging via hydrogen bonding since the polymer has no charge. It is likely that the nonionic state of the polymer does not create strong enough hydrogen bonds with flocs in order to aid COD removal. Also, since the wastewater contains a lot of cations and anions from its inorganic constituents, the lower COD removal can be attributed to the inability of the polymer to neutralize these anions or cations.

Nan et al<sup>102</sup> studied the effect of dosage of nonionic polyacrylamide on flocculation efficiency. They attributed the resulting flocculation to the bridging effect from the amide functional group on nonionic PAM. They observed that low dosage (about 5 ppm) was effective for the removal of particles while high dosages caused crowding and limited contaminant removal. In this research, the dosage effect of nonionic PAM (and further study on this polymer) was however not done, as it was concluded that

the lack of charge on the polymer might reduce the effectiveness of contaminant removal in such highly conductive wastewater.

### 4.3.2 Polyacrylic Acid (PAA)

#### 4.3.2.1 Contaminant removal under acidic condition

Table 4.1 describes contaminant removal with and without PAA under acidic pH (optimized RSM condition).

Contaminants	pH 3.2 (% Removal)	pH 3.2 + PAA (% Removal)
	Batch 2	Batch 2
Fe	53.77	54.61
Ca	27.48	16.98
Cl <sup>-</sup>	45.93	39.91
COD	54.56	58.45

Table 4.1: Contaminant removal in SGPW under optimized RSM conditions

COD and iron removals were slightly improved upon the addition of PAA, but calcium and chloride removal decreased. This can be explained by the pKa of PAA and polymer conformation at different pH. PAA is an anionic polymer mainly due to the negative charge from its carboxyl group. It can participate in charge neutralisation with cations and/or interparticle bridging via hydrogen bonding. It has a pKa of 4.5 below which the  $-COOH$  groups are mostly undissociated<sup>103</sup>. At pH =3, its degree of dissociation is  $0.03^{103}$ , which means that most of the  $-COOH$  groups remain as they are without dissociation. Contaminant removal in this case is mainly through interparticle bridging via hydrogen bonding.

Since pH increases in EC process for an initially acidic wastewater, this increases the amount of  $-COOH$  that are dissociated to  $-COO^-$ . At pH 4.5, degree of dissociation is  $0.5^{103}$ , which means that the amount of bound carboxyl groups equals the number of  $-COO^-$  groups. In this case, both charge neutralization and interparticle bridging via hydrogen bonding occur. Since the final pH for the initially acidic wastewater was around 5 at the end of EC, the combined effect of charge neutralization and interparticle bridging

via hydrogen binding might have contributed to better COD and iron removal observed in acidic condition upon the addition of PAA.

Despite this improvement, calcium and chloride removals were observed to decrease when PAA was added. This might be due to the polymer conformation at this pH. At pH 3, Wisniewska et al<sup>104</sup> reported that PAA adsorbed on a silica oxide/alumina surface in a coil-shaped conformation that enabled the formation of densely packed polymer films. Since positively charged hydroxylated aluminum flocs ( $\text{Al}^{3+}$ ,  $\text{Al}(\text{OH})_2^+$ ,  $\text{Al}(\text{OH})^{2+}$ ) are at a maximum concentration in the acidic pH range<sup>105</sup>, most of the dissociated carboxyl groups interact with the flocs in the coil conformation to neutralize their charge. As a result, adsorption of PAA in this acidic condition has been reported to be high<sup>104,105</sup> due to weak repulsion of  $-\text{COO}^-$  groups. This conformation however limits interaction of contaminants with polymer and flocs. Das et al<sup>105</sup> reported dispersion of contaminants in acidic pH due to crowding of coiled PAA on flocs, leading to steric repulsion and low flocculation at high PAA dosage (10 ppm).

#### 4.3.2.2 Contaminant removal under neutral condition

Table 4.2 describes contaminant removal with and without PAA at neutral pH (preliminary experiment conditions).

Contaminants	pH 7	pH 7+PAA	pH 7	pH 7+PAA
	(%Removal)	(%Removal)	(%Removal)	(%Removal)
	Batch 1	Batch 1	Batch 2	Batch 2
Fe	75.56	72.8	40.41	61.33
Ca	13.66	14.53	26.38	36.64
Cl <sup>-</sup>	20.94	21.91	40.32	52.49
COD	26.37	42.51	56.38	69.78

Table 4.2: Contaminant removal in SGPW under preliminary experiment conditions

Contaminant removal differed between Batch 1 and 2 samples. This is most likely due to the variation in water quality, as wastewater characteristics are known to affect EC performance<sup>89</sup>. It is however evident, as shown in Figure 4.4, that for both types of samples, the addition of PAA boosted contaminant removal (except for iron removal in Batch 1 samples). COD, calcium and chloride showed improved removal when PAA was

added to Batch 1 samples at neutral pH. Iron removal was 3% lower, but was comparatively higher under the same conditions for Batch 2 samples. This could be attributed to the lower concentration of iron in the new wastewater samples (19.24 vs 71.65 mg/L) and the corresponding effect on mass transfer, which might have led to better removal.

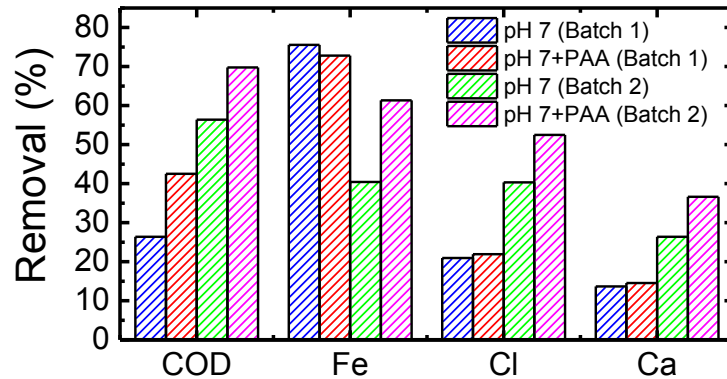


Figure 4.4: Contaminant removal in Batch 1 and 2 samples under neutral pH showing improved removal upon PAA addition

At higher pH such as pH 7, most carboxyl groups on PAA are dissociated and insoluble aluminum hydroxide precipitates also form, whose point of zero charge (pzc) is 8.9<sup>106</sup>. Below this value, the surface-charge of flocs is positive. Dissociated carboxyl groups of PAA can interact with floc surface and form complexes and can also participate in charge neutralization with other ions in the solution. Adsorption of PAA however decreases at higher pH due to strong repulsion among dissociated-COO<sup>-</sup> groups, which leads to a more stretched out conformation of the polymer on the flocs<sup>104</sup>. This enables the interaction of contaminants with resulting flocs and also with unadsorbed polymers, thus significantly improving contaminant removal. Das et al<sup>105</sup> also reported that at high PAA dosage (10 ppm) in a salt solution with alumina, flocculation is at its maximum under alkaline conditions. They attributed this observation to the stretched polymer conformation at neutral pH, which enables bridging and better interaction between polymer and contaminants. A schematic illustrating polymer conformations at different pH is shown in Figure 4.5.

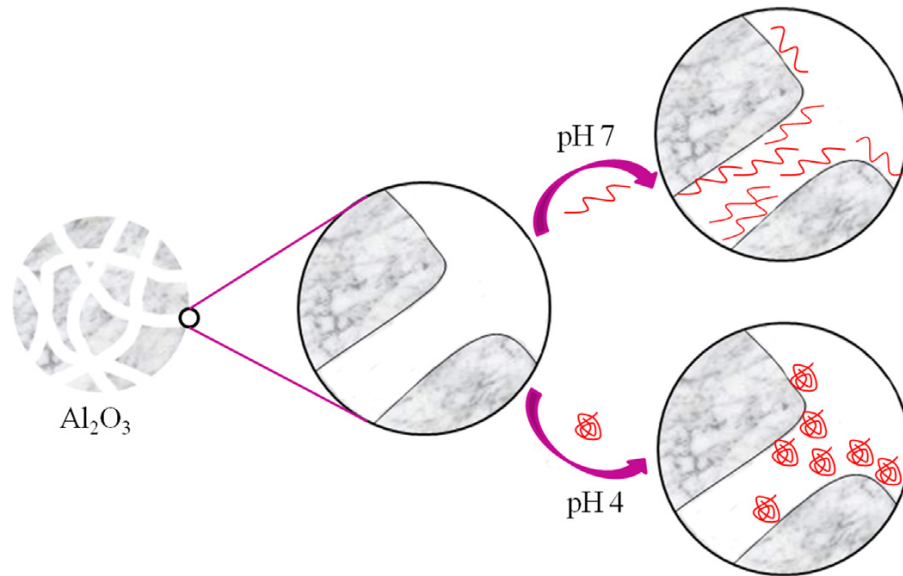


Figure 4.5: PAA conformations under acidic (pH 4) and neutral pH (pH 7)<sup>107</sup>. Under acidic pH, coil conformation is observed on alumina surface while a more stretched out conformation is seen under neutral pH.

It is interesting to note that although a new batch of wastewater samples was used, the RSM optimization is still valid, as the optimum RSM conditions (pH 3.2 without PAA in Table 4.1) showed an overall better removal than the preliminary experiment condition (pH 7 without PAA in Table 4.2). Figure 4.6 illustrates the corresponding COD, calcium, chloride and iron removals for both conditions

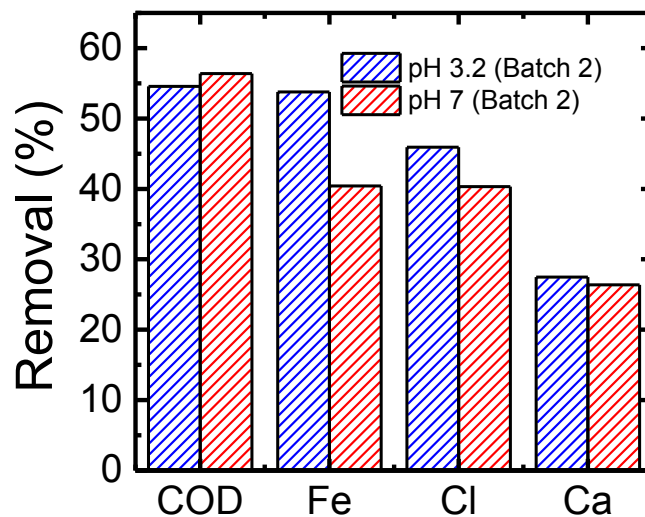


Figure 4.6: Contaminant removals at pH 7 and pH 3.2 for Batch 2 samples (without PAA)

#### 4.4 Sludge Production

Sludge production is also an important factor to consider in any chemical treatment process since it will ultimately affect the downstream cost of the process. An analysis of the sludge generated for each treatment condition, with and without PAA, was done in order to better decide on which EC condition is the most economical and sustainable for industrial application. EC was conducted under four conditions and generated sludge was passed through an 11  $\mu\text{m}$  filter paper. Sludge was placed in an oven at 105°C until all water had evaporated. The weights of the dried sludge were measured and the initial weight of the filter paper was subtracted. Wastewater samples were also treated via conventional chemical coagulation using aluminum sulfate (alum) as coagulant (optimum jar test dosage: 3000 ppm) and its sludge generation was also included for comparison. *Table 4.3* summarizes results from the analysis.

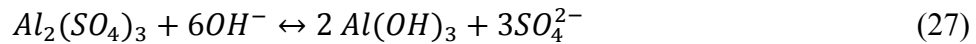
Experiment	EC pretreated WW at pH =3.2	EC pretreated WW at pH =3.2 with 25 ppm PAA	EC pretreated WW at pH =7	EC pretreated WW at pH =7 with 25 ppm PAA	Chemical Coagulation
Sludge generation (kg/m <sup>3</sup> )	0.921	1.901	22.207	56.989	17.923

*Table 4.3: Sludge generation analysis for alum treatment and EC treatments under different conditions*

As expected, the acid condition with no PAA generated the least amount of sludge. The low applied current density contributed to this observation since current density affects the amount of aluminum (and thus floc formation) that dissolves in the solution. When PAA is applied, sludge slightly increases. This is mainly because PAA adsorbs strongly to flocs under acidic pH, and increases floc density and settling. In the neutral condition with no PAA, the large amount of sludge is mainly from the relatively high current density and when PAA is added, sludge increased. Iron also precipitates at

neutral pH and might have also aided removal of other contaminants, thus increasing sludge.

Chemical coagulation with alum generated more sludge than the EC run under acid conditions, but less sludge than the EC run under neutral conditions. This is anticipated and can be explained by calculating the amount of aluminum hydroxide formed for each treatment condition. In the neutral condition, the theoretical amount of aluminum that dissolved to form aluminum hydroxide was calculated to be 5970 mg/L (see *Section 3.3.3.1*). In the acid condition, 1170 mg/L of aluminum dissolved to form aluminum hydroxide (see *Section 3.3.3.2*). In the case of chemical coagulation, according to Equation 27, the theoretical amount of aluminum hydroxide formed from adding 3000 ppm of aluminum sulfate was computed as 1360 mg/L. This is slightly higher than that of the acid condition and less than that of the neutral condition.



#### 4.5 Conclusions

The effect of coagulant aid addition to EC treatment of SGPW was investigated in this chapter. Two types of polymers were examined – nonionic polyacrylamide and anionic polyacrylic acid. Preliminary experiment conditions (pH 7, CD = 200 A/m<sup>2</sup> and 40 minutes reaction time) were employed for the analysis with nonionic polyacrylamide. Preliminary and optimized RSM conditions (pH 3.2, CD = 45 A/m<sup>2</sup> and 35 minutes reaction time) were tested for polyacrylic acid since its degree of ionization varies with pH.

COD removal was not better in the case with nonionic polyacrylamide at neutral pH and improvement in iron removal was only minimal. When polyacrylic acid was used, neutral pH showed better removal of contaminants (Fe: 61.33%, Ca: 36.64%, Cl<sup>-</sup>: 52.49%, COD: 69.78%) compared to the acidic pH condition (Fe: 54.61%, Ca: 16.98%, Cl<sup>-</sup>: 39.91%, COD: 58.45%) for the new wastewater samples. The old wastewater samples also showed the same improvement upon the addition of PAA at neutral pH. This might be due to the stretched out conformation of the polymer at neutral pH and the lesser adsorption propensity of the polymer on the aluminum hydroxide flocs, which creates more room for contaminant interaction (and hence removal) with both flocs and

polymer. In the acidic condition, the reduced efficiency of PAA is probably due to the coiled conformation and strong adsorption of polymer on flocs, both of which hinder interaction of contaminants with flocs.

Sludge production was also evaluated for four EC treatment conditions – pH 3.2, pH 3.2 + PAA, pH 7, and pH 7 + PAA. Sludge from conventional chemical coagulation was also included for comparison. The acid condition (with no PAA) generated the least amount of sludge. This is primarily due to the low current density applied ( $45 \text{ A/m}^2$ ). The pH 7 + PAA case produced the highest amount of sludge not only due to the high current density ( $200 \text{ A/m}^2$ ), but also due to better interaction of contaminants with PAA which causes an increase in floc density. Sludge generation for the chemical coagulation case was intermediate. It was higher than the acid condition (with and without PAA) and lower than both pH 7 conditions. An analysis of the theoretical aluminum hydroxide production (and thus floc generation) for each condition showed that 1170 mg/L, 1360 mg/L and 5970 mg/L of aluminum hydroxide was formed at pH 3, during chemical coagulation with 3000 ppm aluminum sulfate, and at pH 7 respectively. This explains the observation in the sludge generation analysis.

Polyacrylic acid can thus be said to be an effective polymer for the improvement of contaminant removal, especially in the treatment of a highly conductive wastewater like SGPW. The characteristics of the polymer under different pH conditions can be exploited to optimize contaminant removal.

## Chapter 5 – Fouling Reduction Analysis in Forward Osmosis Experiments

### 5.1 Introduction

Forward Osmosis has been employed for wastewater desalination. It is known to have a low fouling propensity and high contaminant rejection. The goal of this chapter is to observe the improvement in fouling reduction of forward osmosis when feed was pretreated under different EC conditions, compared to the cases where raw and chemically coagulated SGPW were applied as feed. Membrane analysis was performed to observe morphology and determine elemental compositions on fouled membrane. Conclusions on the efficiency of EC as a pretreatment for FO were then drawn.

### 5.2 Materials and Methods

#### 5.2.1 Materials

Draw solution was concentrated sodium chloride solution. Sodium chloride was purchased from VWR. Flat sheet, TFC FO membrane was gotten from Porifera. A company in Western Canada provided raw SGPW. Aluminum sulfate was purchased from Fisher Scientific. A conventional jar tester was used for chemical coagulation dosage optimization. Membrane characteristics, as given by company, are summarized in *Table 5.1*.

Water Permeation	$33 \pm 2$ LMH
Reverse Salt Flux	$0.50 \pm 0.2$ g/L
Structural Parameter (S value)	$215 \pm 30$ microns
Max. Trans-Membrane Pressure (TMP)	180 psi
pH operating range	2-11

*Table 5.1: Porifera's TFC membrane specifications*

#### 5.2.2 Experimental setup

A laboratory scale FO cross flow cell was utilized for FO experiments (*Figure 2.6-4*). Effective membrane surface area was  $19.94 \text{ cm}^2$ . Both feed and draw solution tanks were connected to peristaltic pumps that maintained the flow rate of both solutions at 0.5

liters/minute (LPM). The draw solution tank was placed on a digital analytical balance (Model 5102-S, Sartorius, Inc.), which was connected to a computer. The balance was configured to report weight readings every thirty (30) seconds and the change in weight was employed in the calculation of water flux.

### **5.2.3 Methodology**

4.44 M of draw solution was prepared by dissolving 260 grams of sodium chloride in one liter (1 L) of DI water. This concentration was determined based on similar work<sup>46</sup>. Feed solution was also one liter (1 L) of one of the following streams – raw SGPW, SGPW pretreated via EC under optimized RSM condition, SGPW pretreated via EC under optimized RSM condition (+ 25 ppm PAA), SGPW pretreated via EC under preliminary experiment condition, SGPW pretreated via EC under preliminary experiment condition (+ 25 ppm PAA), SGPW pretreated via chemical coagulation. For each condition, except the chemical coagulation treatment, about 1.35 L was treated and stored overnight in order to allow proper settling of sludge. One liter (1 L) of supernatant was then collected and employed as feed.

For chemical coagulation, optimum dosage had to first be determined. Based on Equation 27 and the calculated, theoretical amount of aluminum hydroxide for the optimum RSM condition (1170 mg/L), the theoretical amount of alum needed was determined as 2600 mg/L (rounded to 2 significant figures). Due to limited volume of wastewater, three jars were tested at different alum dosages - 2600, 3000 and 3400 mg/L. 10 g/L of alum was prepared and 260, 300 and 340 ml of alum was added to the corresponding jar. Rapid mixing was done at 95 rpm for about 8 mins and slow mixing was done at 20 rpm for about 12 mins. Addition of alum reduced the pH of the WW below 5. As a result, several drops of 1M sodium hydroxide were added to raise the pH above 5, which is known to be the best pH range for aluminum sulfate. About 20 ml samples were collected and filtered using a 1.5  $\mu\text{m}$  filter paper (GE) prior to turbidity analysis. Samples were diluted 100 times for COD analysis. Optimum aluminum sulfate concentration was then applied to 1 L of SGPW for FO analysis.

Membrane was completely soaked in DI water for at least 24 hours and stored at 4°C. Prior to start of the FO experiment, membrane was positioned in the cell in such a

way that the active layer faced the feed solution. FO runs were conducted for 510 minutes in osmotic dilution mode, which means that the concentration of the draw solution was not maintained over time. Rather, the draw solution became more diluted by the entrance of pure water from the feed. The first hour of the experiment was mainly to allow the system to stabilize and flux readings were calculated after the first hour.

Samples were collected from both feed and draw solutions before and after FO experiments in order to measure change in conductivity. Membranes were dried and stored for further analysis.

### 5.2.4 Analytical Methods

Scanning Electron Microscopy (SEM) (FEI Company, USA) and Energy Dispersive X-ray Spectroscopy (EDAX Octane Super 60 mm<sup>2</sup> SDD) were employed in order to observe the morphology and elemental composition of foulants on the membrane surface. Water flux was analyzed using Equation 13 and the average 15-minute flux was plotted to observe the flux decline over time. Conductivity of both feed and draw solutions was measured using a conductivity meter (Oakton Instruments, Vernon Hills, IL USA) and samples were diluted 100 times prior to conductivity analysis.

## 5.3 Results and Discussion

### 5.3.1 Chemical Coagulation Dosage Optimization

Table 5.2 outlines turbidity and COD results from three jars of 1 L SGPW treated with alum.

Alum concentration (mg/L)	Turbidity (NTU)	% Turbidity reduction	COD (mg/L)	% COD reduction
0	114.1	-	14900	-
2600	7.5	93.42	8180	45.10
3000	2.39	97.90	6580	55.84
3400	4.39	96.15	6340	57.45

Table 5.2: Turbidity and COD reduction for different alum concentrations.

3000 mg/L was chosen as the optimum alum concentration. Turbidity reduction was maximum at this concentration and although COD reduction increased when 3400 mg/L of alum was applied, 3000 mg/L is more economical.

### 5.3.2 Average flux for different feed streams

Table 5.3 summarizes the initial and final flux observed for each feed condition. Figure 5.1 shows the decline in flux over time under different feed conditions.

	% Flux decline	Initial Flux (LMH)	After 450mins (LMH)
Raw	70.16	7.66	2.29
pH 3.2	29.60	5.02	3.53
pH3.2+PAA	37.12	5.30	3.33
pH7	31.40	6.90	4.73
pH7+PAA	27.22	7.22	5.22
Alum	23.53	8.14	6.09

Table 5.3: Initial and final flux data for 450 minutes of FO operation

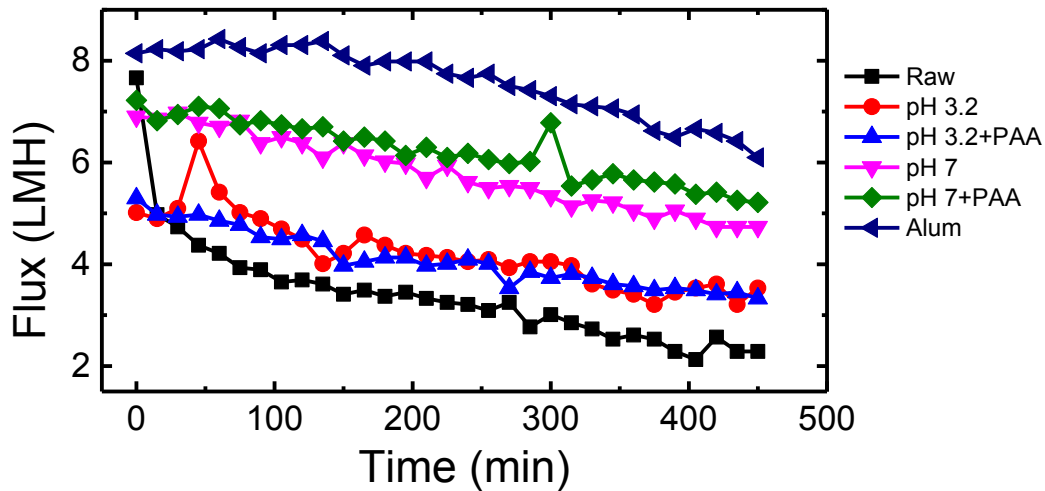


Figure 5.1: Flux trend over 450 minutes of operation for different feed streams

EC treatment enhanced flux stability in the FO and flux decline was not rapid. In the case with no pretreatment, initial flux was very high, but it decreased very quickly within the first 30 minutes after stabilization and final flux was about 2 LMH. Flux decline was about 70% at 450 minutes. Hickenbottom et al<sup>46</sup> also reported an even higher initial flux

(14 LMH) using raw drilling mud wastewater from fracking operations, but similarly, flux reduced to 2 LMH by six hours of operation. The high initial flux for the raw feed, compared to other feed streams, can be attributed to the corresponding high osmotic pressure difference between the raw feed and draw solution. *Table 5.4* reports the initial feed and draw conductivity measurements for different feed streams. Except for the alum-treated feed, the raw feed had the highest difference in conductivity between feed and draw solutions.

	Conductivity (mS)		
	Draw solution	Feed solution	% Difference
Raw	799	628	21.40
pH 3.2	770	640	16.88
pH 3.2 + PAA	746	662	11.26
pH 7	765	626	18.17
pH 7 + PAA	806	663	17.74
Alum	815	513	37.06

*Table 5.4: Conductivities of initial draw and feed solutions*

When EC pretreatment was applied, flux decline ranged from 27%-37% at 450 minutes. The conductivities of the EC treated feeds (except at pH 7) were higher than the raw feed most likely due to residual aluminum and/or PAA in the solution. This might have led to lower osmotic pressure difference and thus a lower initial flux compared to the raw feed. When PAA was added, the initial feed conductivity increased compared to the case with no PAA and as a result, the percent difference in conductivity for feeds treated with PAA was less than those without PAA. However, one would expect that the initial flux would be lower for treatments with PAA (since perhaps there is residual PAA in the solution and the % difference in conductivity is lower), but this is not the case. Higher initial fluxes were observed for feeds treated with PAA. This might result from the interaction between membrane properties and feed solution. Since some PAA exists in ionic form around pH 5-6.5 (final pH range for both acid and neutral condition), they would be repelled by the negatively charged TFC membrane. Thus, residual PAA in the solution might have interacted with contaminants by forming complexes and hindered the

initial fouling of the membrane. Blandin et al<sup>108</sup> also observed high rejection of trace organic compounds using Porifera’s TFC membrane compared to two other membranes. The authors attributed this to the negative charge of the membrane that allows the repulsion of negatively charged compounds, among other reasons.

In specifically analyzing results for each feed, the pH 3.2 condition showed higher final flux compared to the pH 3.2+PAA condition. This aligns with findings and discussion in *Section 4.3.2.1*, where lower contaminant removal was observed upon the addition of PAA due to high adsorption on floc surface and coiled conformation of polymer. For the neutral conditions, initial and final flux were higher than acid conditions (with and with and without PAA). pH 7+ PAA showed the least flux decline, as in *Section 4.3.2.2*, COD and ion removal was highest in the pH 7+PAA case due to lesser adsorption and more stretched-out conformation of polymer.

The treatment with chemical coagulation reported the lowest initial feed conductivity. This might be due to the formation of long chain, complex, positively charged aluminum hydroxide species ( $Al_{13}(OH)_{34}^{5+}$ ) at the optimum pH range for alum. At pH 3.2 and 7 (for the EC pretreatment), the formation of such polymeric species is possible but they are transformed quickly to monomeric species ( $Al(OH)^{2+}$ ,  $Al(OH)^{+}_2$ ) at pH 3.2 and/or aluminum hydroxide precipitates ( $Al(OH)_3$ ) at pH 7. *Table 5.5* illustrates that removal of studied contaminants was least when chemical coagulation treatment was applied. Thus, it can be said that these long-chain aluminum hydroxide species, generated when alum was employed, might have been effective for better removal of other contaminants besides those explored in this study.

	% Removal			
	COD	Ca	Fe	Cl <sup>-</sup>
pH 3.2	54.56	27.48	53.77	45.93
pH 7+PAA	69.78	36.64	61.33	52.49
Alum	55.84	27.71	38.27	25.06

*Table 5.5: Contaminant removal after chemical coagulation and EC treatment under two different pH conditions*

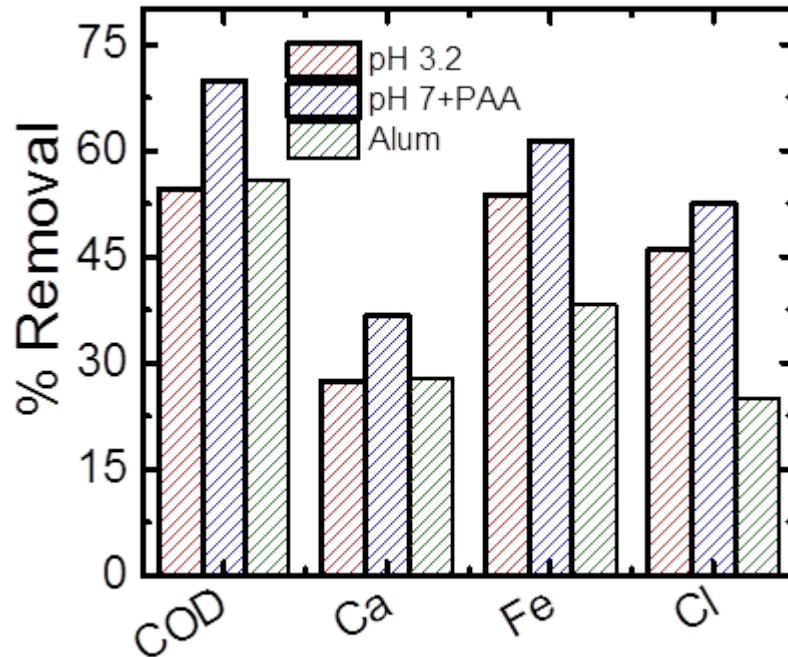


Figure 5.2: Graphical comparison of COD and ion removal in EC and alum pretreatment

Alum treatment also showed the highest initial and final flux. The high initial flux is most likely due to the initial osmotic pressure difference, which is highest in the case with alum. Flux decline was least (about 23%) and the final flux was highest. One major difference between the alum treated feed and those treated via EC is that a large amount of sulfate ions is produced upon dissolution of alum. For each mole of alum, three moles of sulfate ion is produced (theoretically, 3000 ppm alum generates about 2500 mg/L of sulfate). As a result, the flux trend, observed in the case of alum, can be analyzed in terms of the significant presence of sulfate ion.

The presence of a high concentration of calcium and sulfate ions can lead to the formation of a well-known scale – gypsum (calcium sulfate dehydrate). Calcium carbonate is another scale that could also form. One would expect significant fouling in the treatment with alum since the water quality is suitable for gypsum formation on the membrane surface. Nevertheless, this was not the case and to explain this, an understanding on the mechanism of gypsum formation is necessary. This mechanism is also similar to that of calcium carbonate scale formation.

Gypsum can form either by bulk precipitation and deposition on membrane or by direct crystallization on membrane surface<sup>109</sup> (Figure 5.3).

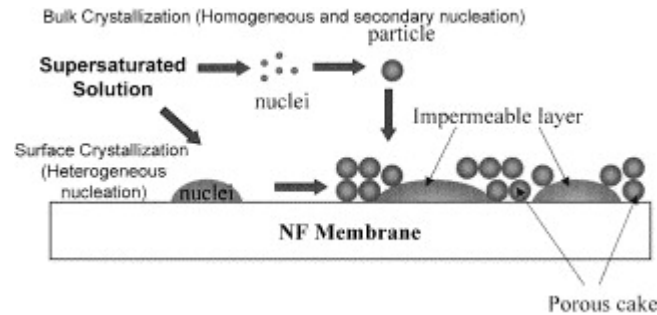


Figure 5.3: Mechanism of gypsum scale formation (although figure describes scale formation on a nanofiltration membrane, mechanism is also applicable to FO membrane)<sup>109</sup>

In the bulk mechanism, crystals are formed in the solution and deposit on the membrane surface. The reduction in flux thus results from the accumulation of these deposits or layers on the membrane with time. Mi et al<sup>110</sup>, in their work, cite a similar mechanism proposed by other researchers for the formation of calcium carbonate crystals. This mechanism involves the creation of prenucleation bundles, which later assemble to form amorphous nanoparticles (size around 20-70 nm). These nanoparticles later become polycrystals of larger size (100-500 nm), which later deposit on the membrane surface, after attaining a certain, critical size. The authors highlight that this mechanism is not limited to only calcium carbonate crystal formation but to others like gypsum. In the surface crystallization mechanism, a nucleus is formed directly on the membrane surface, which grows to form crystals.

Both mechanisms could occur especially if the solution is supersaturated; however, Dydo et al<sup>111</sup> highlight that most research point mainly to the bulk mechanism for the formation of gypsum scale. It is therefore important to note that in the bulk mechanism, the formation of crystals in the solution involves a time factor for nuclei growth, crystal formation, accumulation on membrane and thus membrane fouling<sup>111-113</sup>. Mi et al<sup>110</sup> conducted a study on gypsum scaling using synthetic wastewater (35 mM CaCl<sub>2</sub>, 20 mM Na<sub>2</sub>SO<sub>4</sub> and 19 mM NaCl). Corresponding sulfate concentration was about 1921 mg/L. They used two types of membrane – CTA and TFC – and membrane

was positioned in such a way that the active layer facing feed. FO experiment was also performed in osmotic dilution mode. They observed gradual flux decline for both membranes, but after 48 hours, a sharp flux decline (from 2 LMH to almost 0 LMH) was observed for the TFC membrane. Shirazi et al<sup>112</sup> also studied  $\text{Ca}_2\text{SO}_4$  and  $\text{CaHPO}_4$  fouling on nanofiltration membranes. Calcium sulfate concentration in the solution was 2000 mg/L. They observed that flux was steady for 4.5 hours after which flux declined rapidly. They also pointed out that nucleation was slow in the case of  $\text{Ca}_2\text{SO}_4$  fouling. Colburn et al<sup>114</sup> also observed no significant gypsum fouling on their nanofiltration membranes, although the wastewater had relatively high concentrations of calcium and sulfate (Initial sulfate concentration was 1169 mg/L and final concentration in retentate was about 1600 mg/L). They agree that indeed some gypsum is formed in the solution, but it does not attach to the membrane surface since no major flux decline was observed. They highlight that more study is necessary to determine and compare the rate of flux decline when gypsum precipitates in the solution or on the membrane surface.

Other factors are also known to delay or hinder the formation of gypsum scale on the membrane. Since sulfate is a divalent anion, its significant presence in the feed requires the presence of divalent and monovalent cations such as calcium and sodium to keep charge neutrality on the feed side. As a result, the migration of calcium and sodium (and thus membrane fouling due to these ions) is limited<sup>115</sup>. Presence of high concentrations of magnesium, chloride, bicarbonate and sodium ions has been reported to increase gypsum solubility and thus hinder its crystallization<sup>114,116</sup>. Also, competition among these ions (for example in the case of bicarbonate, magnesium and sodium ions) might retard gypsum and calcium carbonate scale formation. Rahardianto et al<sup>113</sup> did not observe calcium carbonate precipitates on membrane surface even after 24 hours of RO operation. They attributed this to the time lag in crystal formation. They expect that ultimately, as gypsum saturates in the solution and bicarbonate concentration increases, calcium carbonate deposits would form on the membrane. It can thus be concluded that for SGPW treatment with alum, the formation of gypsum and other scale like calcium carbonate might have occurred after a much longer period of time than that of the present study (>9 hours) and the effect on flux might have been more significant.

The presence of high amount of sulfate in the final concentrated feed can be problematic. To lower sulfate concentration to acceptable levels, anaerobic treatments have been employed as they are effective and overcome the shortcomings of other biological and physicochemical treatments<sup>117</sup>. However, the high concentration of sulfate limits anaerobic treatment due to the generation of toxic H<sub>2</sub>S.

For all treatments, flux declined over time due to concentration polarization and reduced osmotic pressure difference.

### 5.3.3 Membrane Analysis

Figure 5.4 compares SEM images for virgin membranes and three different feed conditions - raw, pH 3.2, and pH 7 +PAA

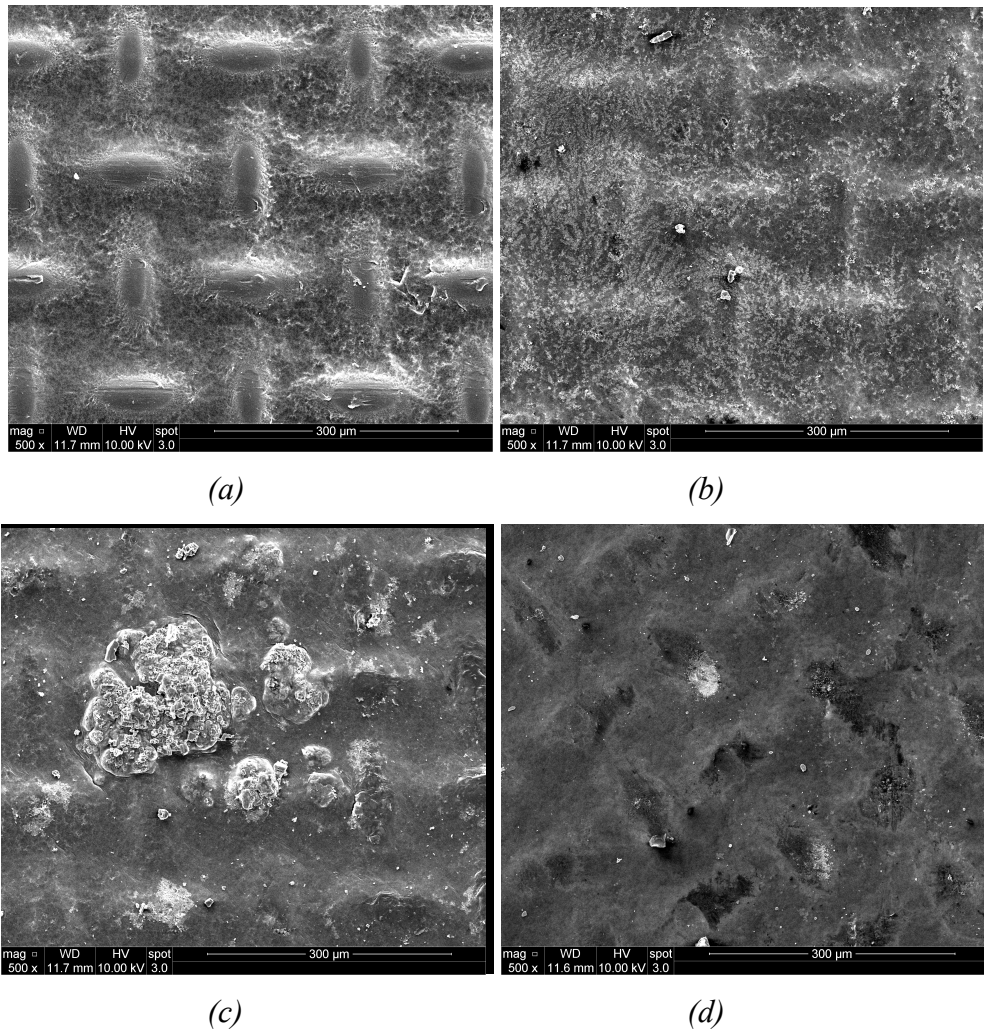


*Figure 5.4: (a) SEM for virgin TFC membrane; Fouling observations on TFC membrane (b) when raw SGPW was employed as feed; (c) when SGPW, treated via EC at pH 3.2, time 35 mins and current density 45 A/m<sup>2</sup>, was employed as feed; (d) when SGPW, treated via EC at pH 7, time 40 mins and current density 200 A/m<sup>2</sup> with PAA, was employed as feed.*

Elemental analysis of the pristine TFC membrane showed no contaminants. However, when different pretreated wastewater (including the raw wastewater) were employed as feed, varying percentages of different inorganics such as calcium, chloride, magnesium, sodium, aluminum and barium were observed on the membrane surface. Large crystals (in (c) for example) is mainly from sodium chloride, as drying the membrane leads to its crystallization. Significant percentages of carbon and oxygen were also reported. This points to the possible formation of calcium carbonate on the membrane. It is however difficult to attribute the presence of carbon and oxygen on fouled membranes to organic fouling since the pristine membrane is also made up of carbon and oxygen.

#### **5.4 Conclusions**

In this section, flux reduction and membrane fouling in FO were observed for different pretreated SGPW streams. Feed was treated via electrocoagulation under acidic and neutral conditions, with and without PAA, and 4.44 M sodium chloride solution was used as the draw solution. The resulting flux was compared to the cases with raw and alum treated (optimum dosage: 3000 mg/L) feed. Results showed that EC reduced the rate of flux decline to 27-37% at 450 minutes compared to 70% flux decline for the raw SGPW feed. Also, flux trend agreed with contaminant removal analysis in Chapter 4 for different EC treatment conditions, with and without PAA. EC pretreatment at pH 3.2 (with no PAA) had shown better COD, iron, chloride and calcium removal compared to the case with PAA. Consequently, flux was higher in the case with no PAA. Similarly, EC pretreatment at pH 7+PAA had shown better COD, iron, chloride and calcium removal than the case with no PAA. Hence, flux decline was lower in the case with PAA.

Interestingly, alum pretreatment showed the highest initial and final flux. In spite of its poor removal of the contaminants investigated in this thesis, alum pretreatment reported the least initial conductivity, which led to a high initial flux. This reduction in

conductivity can be attributed to the formation of polymeric aluminum hydroxide species compared to monomeric species and precipitates formed in the EC pretreatment conditions. Alum pretreated feed also reported the least flux decline (23%). Since alum generates a large amount of sulfate ions and SGPW has a high concentration of calcium ions, gypsum (calcium sulfate dihydrate) scale was expected to deposit on the membrane and cause flux to decline. However, within the 450-minute time frame, significant scale formation was not observed. This is mainly because gypsum requires adequate time for nuclei growth, crystal formation, and accumulation on membrane. Other plausible reasons for the delay in gypsum scaling include increased gypsum solubility due to the presence of high concentrations of magnesium, chloride, bicarbonate and sodium ions and competition among these ions for the formation of other compounds. It can thus be concluded that for SGPW treatment with alum, the formation of gypsum and other scale like calcium carbonate and the corresponding effect on flux might have occurred after a much longer period of time than that of the present study (>9 hours).

For EC pretreatments, these two conditions showed the least flux decline - pH 3.2 without PAA, and pH 7+PAA. The latter showed a higher final flux (5.22 vs 3.53 LMH) at 450 minutes, similar to its better contaminant removal observed in Chapter 4.

## Chapter 6 - Conclusions and Recommendations

In this thesis, electrocoagulation was studied for the treatment of SGPW, specifically for COD reduction and removal of calcium, iron and chloride ions, in order to minimize fouling in FO. In Chapter 3, preliminary experiments using synthetic wastewater and response surface methodology optimization using industrial wastewater were performed in order to establish EC conditions that showed best contaminant removal. In Chapter 4, the effect of the addition of a coagulant aid to EC was explored. It was hypothesized that the addition of coagulant aid to the EC process will improve contaminant removal. Anionic polyacrylic acid and nonionic polyacrylamide were tested under the optimized RSM condition and also the preliminary experiment condition. In Chapter 5, improved fouling reduction in the FO process for different pretreated and non-pretreated SGPW feed streams was investigated. Feed was treated via electrocoagulation under acidic and neutral conditions, with and without PAA, and also with alum for comparison. Conclusions from this study are summarized below:

- EC pretreatment under pH 3.2 condition is the most desirable for an industry looking to reuse its wastewater primarily because it generates the least sludge and based on results from this study, concentrations of iron, calcium, chloride and COD can be reduced to 8.85, 14375, 46656, and 6705 mg/L, respectively (from an initial 19.24, 19692, 86400, and 14900 mg/L, respectively). These correspond to 54.61% iron removal, 16.98% calcium removal, 39.91% chloride removal, and 58.45% COD removal. TDS was reduced to 4800 mg/L, which is below the desired concentration in *Table 6.1*. Although calcium concentration is still high, the pretreated water is still suitable for direct reuse for fracking operations since its chloride concentration, which is typically the highest for the studied wastewater, was significantly reduced via EC pretreatment.

Bacteria	100,000 per 100 ml
Barium (mg/l)	< 2
Bicarbonates (mg/l)	250 to 100,000
Calcium (mg/l)	300
Chlorides (mg/l)	2,000 to 40,000
Iron (mg/l)	10
Hydrogen sulfide (mg/l)	ND
Magnesium (mg/l)	100
pH	6.5 to 8.0
Phosphates (mg/l)	10
Radionuclides (pCi/l)	<15
Reducing agents (mg/l)	ND
Silica (mg/l)	<20
Strontium (mg/l)	<10
Sulfate (mg/l)	400 to 1,000
Total Dissolved Solids (mg/l)	500 to 5,000

Table 6.1: Desired water quality for hydraulic fracturing<sup>18</sup>

- EC pretreatment under pH 7 (with the addition of 25 ppm PAA) further improves the quality of the product water. Final concentrations of iron, calcium, chloride and COD were 7.5, 12406, 41472, 4470 mg/L, respectively. These correspond to 61.33% iron removal, 36.64% calcium removal, 52.49% chloride removal, 69.78% COD removal. TDS was reduced to 4710 mg/L, which is also below the desired concentration in *Table 6.1*. The major drawback to the implementation of this treatment condition might be sludge generation and management, which is nevertheless an issue that is faced in any type of wastewater treatment. It is therefore suggested that this pretreatment condition be employed mainly if FO membrane treatment is employed after pretreatment. This is because EC pretreatment at pH 7 (+ 25 ppm PAA) can maintain a high, stabilized flux over time, based on findings from this study.
- There is no need for filtration after EC, as sludge can be allowed to settle in a tank and supernatant can be continuously extracted to the FO system. Chemical coagulation with alum is not recommended due to the excessive use of chemicals, high sulfate concentration in feed and reported sharp flux decline after 2 days of operation, according to literature, due to gypsum scale formation on membrane. EC pretreatment reduced the rate of flux decline to 27-37% at 450 minutes

compared to 70% flux decline for the raw SGPW feed. Also, EC pretreated feed at neutral pH, with PAA, showed the least flux decline (27%), followed by the EC pretreated feed at acidic pH, with no PAA (29%).

Future recommendations based on work done in this study include:

- **Investigation of EC pretreatment under pH 7 + 25 ppm PAA at a lower current density (e.g. 45 A/m<sup>2</sup>)** – The resulting effect on contaminant removal and sludge production can be studied to compare removal efficiencies at different current densities upon the addition of PAA.
- **Integration and analysis of a draw solution regeneration system** – This aspect was not investigated in this thesis. Since the draw solution becomes more diluted over time, membrane processes like reverse osmosis and membrane distillation can be employed to regenerate draw solute and extract pure water. Researchers have explored the application of these two processes for draw solution regeneration<sup>119,120</sup>.
- **Investigation of sludge management options** – The only limitation for the EC (pH 7 + 25 ppm PAA)-FO hybrid implementation might be sludge generation from pretreatment stage. As a result, effective solutions for sludge management should be studied.
- **Flux recovery due to membrane cleaning** – Although not explored in this thesis, membrane cleaning such as osmotic backwashing has been reported to improve the flux<sup>121</sup>. It would be insightful to observe the degree of flux recovery when membrane cleaning is applied during SGPW treatment.
- **Long-term FO fouling test** – This timeframe for this study was only limited to 9 hours. A longer period of time for FO test after pretreatment would be helpful to better analyze fouling on the FO membrane. Possible effects of different operating conditions such as temperature and cross-flow velocity can also be explored.

## References

1. Kondash, A.; Vengosh, A. Water Footprint of Hydraulic Fracturing. *Environmental Science & Technology Letters* **2015**, *2*, 276-280.
2. Stringfellow, W. T.; Domen, J. K.; Camarillo, M. K.; Sandelin, W. L.; Borglin, S. Physical, chemical, and biological characteristics of compounds used in hydraulic fracturing. *Journal of Hazardous Materials* **2014**, *275*, 37-54.
3. Jackson, R. B.; Vengosh, A.; Carey, J. W.; Davies, R. J.; Darrah, T. H.; O'sullivan, F.; Pétron, G. The environmental costs and benefits of fracking. *Annual Review of Environment and Resources* **2014**, *39*, 327-362.
4. GWPC, I. Hydraulic Fracturing: The Process. <https://fracfocus.org/hydraulic-fracturing-how-it-works/hydraulic-fracturing-process> (2017).
5. Chen, H.; Carter, K. E. Water usage for natural gas production through hydraulic fracturing in the United States from 2008 to 2014. *Journal of Environmental Management* **2016**, *170*, 152-159.
6. Ferrer, I.; Thurman, E. M. Chemical constituents and analytical approaches for hydraulic fracturing waters. *Trends in Environmental Analytical Chemistry* **2015**, *5*, 18-25.
7. USEPA The Hydraulic Fracturing Water Cycle. <https://www.epa.gov/hfstudy/hydraulic-fracturing-water-cycle>; (accessed 12/16, 2016).
8. Zhao, S.; Huang, G.; Cheng, G.; Wang, Y.; Fu, H. Hardness, COD and turbidity removals from produced water by electrocoagulation pretreatment prior to Reverse Osmosis membranes. *Desalination* **2014**, *344*, 454-462.
9. Goss, G.; Alessi, D.; Allen, D.; Gehman, J.; Brisbois, J.; Kletke, S.; Zolfaghari, A.; Notte, C.; Thompson, Y.; Hong, K. Unconventional wastewater management: a comparative review and analysis of hydraulic fracturing wastewater management practices across four North American basins. **2015**.
10. Encana Corporation 2013 Sustainability Report. **2013**.
11. Kuokkanen, V.; Kuokkanen, T. Recent applications of electrocoagulation in treatment of water and wastewater—a review. *Green and Sustainable Chemistry* **2013**, *3*, 89-121.
12. Sari, M. A.; Chellam, S. Mechanisms of boron removal from hydraulic fracturing wastewater by aluminum electrocoagulation. *Journal of Colloid and Interface Science* **2015**, *458*, 103-111.

13. McCutcheon, J. R.; McGinnis, R. L.; Elimelech, M. A novel ammonia—carbon dioxide forward (direct) osmosis desalination process. *Desalination* **2005**, *174*, 1-11.
14. Moreno-Casillas, H. A.; Cocke, D. L.; Gomes, J. A. G.; Morkovsky, P.; Parga, J. R.; Peterson, E. Electrocoagulation mechanism for COD removal. *Separation and Purification Technology* **2007**, *56*, 204-211.
15. Ukiwe, L.; Ibeneme, S.; Duru, C.; Okolue, B.; Onyedika, G.; Nweze, C. Chemical and Electrocoagulation Techniques in Coagulation-Flocculation in Water and Wastewater Treatment—a Review. *International Journal of Research and Reviews in Applied Sciences* **2014**, *18*, 1.
16. Verma, A. K.; Dash, R. R.; Bhunia, P. A review on chemical coagulation/flocculation technologies for removal of colour from textile wastewaters. *Journal of Environmental Management* **2012**, *93*, 154-168.
17. Vengosh, A.; Jackson, R. B.; Warner, N.; Darrah, T. H.; Kondash, A. A Critical Review of the Risks to Water Resources from Unconventional Shale Gas Development and Hydraulic Fracturing in the United States. *Environmental Science & Technology* **2014**, *48* (15), 8334–8348.
18. Rabinowitz, P. M.; Slizovskiy, I. B.; Lamers, V.; Trufan, S. J.; Holford, T. R.; Dziura, J. D.; Peduzzi, P. N.; Kane, M. J.; Reif, J. S.; Weiss, T. R.; Stowe, M. H. Proximity to natural gas wells and reported health status: results of a household survey in Washington County, Pennsylvania. *Environmental Health Perspectives* **2015**, *123*, 21-26.
19. Moritz, A.; Hélie, J.; Pinti, D. L.; Larocque, M.; Barnette, D.; Retailleau, S.; Lefebvre, R.; Gélinas, Y. Methane baseline concentrations and sources in shallow aquifers from the shale gas-prone region of the St. Lawrence Lowlands (Quebec, Canada). *Environmental Science & Technology* **2015**, *49*, 4765-4771.
20. Alessi, D. S.; Zolfaghari, A.; Kletke, S.; Gehman, J.; Allen, D. M.; Goss, G. G. Comparative analysis of hydraulic fracturing wastewater practices in unconventional shale development: Water sourcing, treatment and disposal practices. *Canadian Water Resource Journal/Revue Canadienne des Ressources Hydriques* **2017**, *42*, 105-121.
21. Monika, F. Hydraulic Fracturing & Water Stress: Water Demand by the Numbers. Shareholder, Lender & Operator Guide to Water Sourcing. *Ceres* **2014**.
22. Frohlich, C.; Brunt, M. Two-year survey of earthquakes and injection/production wells in the Eagle Ford Shale, Texas, prior to the MW4.8 20 October 2011 earthquake. *Earth and Planetary Science Letters* **2013**, *379*, 56-63.

23. Howarth, R. W.; Ingraffea, A.; Engelder, T. Natural gas: Should fracking stop? *Nature* **2011**, *477*, 271-275.
24. Ferrar, K. J.; Michanowicz, D. R.; Christen, C. L.; Mulcahy, N.; Malone, S. L.; Sharma, R. K. Assessment of effluent contaminants from three facilities discharging Marcellus Shale wastewater to surface waters in Pennsylvania. *Environmental Science & Technology* **2013**, *47*, 3472-3481.
25. Bulletin, P. Rules and Regulations, Title 25 - Environmental Protection, Environmental Quality Board [25 PA. CODE CH. 95 ], Wastewater Treatment Requirements. <http://www.pabulletin.com/secure/data/vol40/40-34/1572.html> (accessed August 21, 2010).
26. Rahm, B. G.; Bates, J. T.; Bertoia, L. R.; Galford, A. E.; Yoxtheimer, D. A.; Riha, S. J. Wastewater management and Marcellus Shale gas development: Trends, drivers, and planning implications. *Journal of Environmental Management* **2013**, *120*, 105-113.
27. Abdalla, C.; Drohan, J.; Rahm, B.; Jacquet, J.; Becker, J.; Collins, A.; Klaiber, H. A.; Poe, G.; Grantham, D. Water's journey through the shale gas drilling and production processes in the Mid-Atlantic Region. *Penn State Extension: College of Agricultural Sciences, Penn State* **2012**.
28. QOGA Quebec Government gives the first authorization certificate for fracking in Quebec. <http://www.apgq-qoga.com/en/2016/06/21/quebec-government-gives-the-first-authorization-certificate-for-fracking-in-quebec/> (accessed 06/21, 2016).
29. Becklumb, P.; Chong, J.; Williams, T. *Shale Gas in Canada: Environmental Risks and Regulation*; 2015; Vol. 18-E.
30. Guerra, K.; Dahm, K.; Dundorf, S. Oil and gas produced water management and beneficial use in the Western United States. **2011**, 157.
31. Igunnu, E. T.; Chen, G. Z. Produced water treatment technologies. *International Journal of Low-Carbon Technologies* **2012**, *9*, 157-177.
32. McGinnis, R. L.; Hancock, N. T.; Nowosielski-Slepowron, M. S.; McGurgan, G. D. Pilot demonstration of the NH<sub>3</sub>/CO<sub>2</sub> forward osmosis desalination process on high salinity brines. *Desalination* **2013**, *312*, 67-74.
33. Fakhru'l-Razi, A.; Pendashteh, A.; Abdullah, L. C.; Biak, D. R. A.; Madaeni, S. S.; Abidin, Z. Z. Review of technologies for oil and gas produced water treatment. *Journal of Hazardous Materials* **2009**, *170*, 530-551.

34. Cho, H.; Jang, Y.; Koo, J.; Choi, Y.; Lee, S.; Sohn, J. Effect of pretreatment on fouling propensity of shale gas wastewater in membrane distillation process. *Desalination and Water Treatment* **2016**, *57*, 24566-24573.
35. Wang, W.; Yan, X.; Zhou, J.; Ma, J. Treatment of hydraulic fracturing wastewater by wet air oxidation. *Water Science and Technology* **2016**, *73*, 1081-1089.
36. Rosenblum, J. S.; Sitterley, K. A.; Thurman, E. M.; Ferrer, I.; Linden, K. G. Hydraulic fracturing wastewater treatment by coagulation-adsorption for removal of organic compounds and turbidity. *Journal of Environmental Chemical Engineering* **2016**, *4*, 1978-1984.
37. Lobo, F. L.; Wang, H.; Huggins, T.; Rosenblum, J.; Linden, K. G.; Ren, Z. J. Low-energy hydraulic fracturing wastewater treatment via AC powered electrocoagulation with biochar. *Journal of Hazardous Materials* **2016**, *309*, 180-184.
38. Haydar, S.; Aziz, J. A. Coagulation–flocculation studies of tannery wastewater using combination of alum with cationic and anionic polymers. *Journal of Hazardous Materials* **2009**, *168*, 1035-1040.
39. Aguilar, M.; Saez, J.; Lloréns, M.; Soler, A.; Ortuno, J.; Meseguer, V.; Fuentes, A. Improvement of coagulation–flocculation process using anionic polyacrylamide as coagulant aid. *Chemosphere* **2005**, *58*, 47-56.
40. Un, U. T.; Koparal, A. S.; Ogutveren, U. B. Electrocoagulation of vegetable oil refinery wastewater using aluminum electrodes. *Journal of Environmental Management* **2009**, *90*, 428-433.
41. Irfan, M.; Butt, T.; Imtiaz, N.; Abbas, N.; Khan, R. A.; Shafique, A. The removal of COD, TSS and colour of black liquor by coagulation–flocculation process at optimized pH, settling and dosing rate. *Arabian Journal of Chemistry* **2013**, *10*, S2307-S2318.
42. Aguilar, M.; Saez, J.; Llorens, M.; Soler, A.; Ortuno, J. Microscopic observation of particle reduction in slaughterhouse wastewater by coagulation–flocculation using ferric sulphate as coagulant and different coagulant aids. *Water Research* **2003**, *37*, 2233-2241.
43. Roy, D.; Rahni, M.; Pierre, P.; Yargeau, V. Forward osmosis for the concentration and reuse of process saline wastewater. *Chemical Engineering Journal* **2016**, *287*, 277-284.
44. Bell, E. A. Long-term fouling and performance of forward osmosis membranes treating activated sludge and oil and gas produced water, Colorado School of Mines, United States -- Colorado, 2015.

45. Zhao, P.; Gao, B.; Yue, Q.; Liu, S.; Shon, H. K. Effect of high salinity on the performance of forward osmosis: Water flux, membrane scaling and removal efficiency. *Desalination* **2016**, *378*, 67-73.
46. Hickenbottom, K. L.; Hancock, N. T.; Hutchings, N. R.; Appleton, E. W.; Beaudry, E. G.; Xu, P.; Cath, T. Y. Forward osmosis treatment of drilling mud and fracturing wastewater from oil and gas operations. *Desalination* **2013**, *312*, 60-66.
47. Shaffer, D. L.; Arias Chavez, L. H.; Ben-Sasson, M.; Romero-Vargas Castrillón, S.; Yip, N. Y.; Elimelech, M. Desalination and reuse of high-salinity shale gas produced water: drivers, technologies, and future directions. *Environmental Science & Technology* **2013**, *47*, 9569-9583.
48. Coday, B. D.; Xu, P.; Beaudry, E. G.; Herron, J.; Lampi, K.; Hancock, N. T.; Cath, T. Y. The sweet spot of forward osmosis: treatment of produced water, drilling wastewater, and other complex and difficult liquid streams. *Desalination* **2014**, *333*, 23-35.
49. Coday, B. D.; Almaraz, N.; Cath, T. Y. Forward osmosis desalination of oil and gas wastewater: Impacts of membrane selection and operating conditions on process performance. *Journal of Membrane Science* **2015**, *488*, 40-55.
50. Ozyonar, F.; Aksoy, S. Removal of Salicylic Acid from Aqueous Solutions Using Various Electrodes and Different Connection Modes by Electrocoagulation. *International Journal of Electrochemical Science* **2016**, *11*, 3680-3696.
51. Kariyajjanavar, P.; Narayana, J.; Nayaka, Y. Degradation of Textile Wastewater by Electrochemical Method. *Hydrology: Current Research* **2011**, *2*.
52. Safari, S.; Aghdam, M. A.; Kariminia, H. Electrocoagulation for COD and diesel removal from oily wastewater. *International Journal of Environmental Science and Technology* **2016**, *13*, 231-242.
53. Feng, J.; Sun, Y.; Zheng, Z.; Zhang, J.; Shu, L.; Tian, Y. Treatment of tannery wastewater by electrocoagulation. *Journal of Environmental Sciences* **2007**, *19*, 1409-1415.
54. Zhu, J.; Wu, F.; Pan, X.; Guo, J.; Wen, D. Removal of antimony from antimony mine flotation wastewater by electrocoagulation with aluminum electrodes. *Journal of Environmental Sciences* **2011**, *23*, 1066-1071.
55. Mechelhoff, M.; Kelsall, G. H.; Graham, N. J. Electrochemical behaviour of aluminium in electrocoagulation processes. *Chemical Engineering Science* **2013**, *95*, 301-312.

56. Vasudevan, S.; Lakshmi, J.; Packiyam, M. Electrocoagulation studies on removal of cadmium using magnesium electrode. *Journal of Applied Electrochemistry* **2010**, *40*, 2023-2032.
57. Ganesan, P.; Lakshmi, J.; Sozhan, G.; Vasudevan, S. Removal of manganese from water by electrocoagulation: adsorption, kinetics and thermodynamic studies. *The Canadian Journal of Chemical Engineering* **2013**, *91*, 448-458.
58. Vasudevan, S.; Sheela, S. M.; Lakshmi, J.; Sozhan, G. Optimization of the process parameters for the removal of boron from drinking water by electrocoagulation—a clean technology. *Journal of Chemical Technology and Biotechnology* **2010**, *85*, 926-933.
59. Oumar, D.; Patrick, D.; Gerardo, B.; Rino, D.; Ihsen, B. S. Coupling biofiltration process and electrocoagulation using magnesium-based anode for the treatment of landfill leachate. *Journal of Environmental Management* **2016**, *181*, 477-483.
60. Hakizimana, J. N.; Gourich, B.; Chafi, M.; Stiriba, Y.; Vial, C.; Drogui, P.; Naja, J. Electrocoagulation process in water treatment: A review of electrocoagulation modeling approaches. *Desalination* **2017**, *404*, 1-21.
61. Esmaelirad, N.; Carlson, K.; Ozbek, P. O. Influence of softening sequencing on electrocoagulation treatment of produced water. *Journal of Hazardous Materials* **2015**, *283*, 721-729.
62. Feng, Y.; Yang, L.; Liu, J.; Logan, B. E. Electrochemical technologies for wastewater treatment and resource reclamation. *Environmental Science: Water Research & Technology* **2016**, *2*, 800-831.
63. Malakootian, M.; Mansoorian, H.; Moosazadeh, M. Performance evaluation of electrocoagulation process using iron-rod electrodes for removing hardness from drinking water. *Desalination* **2010**, *255*, 67-71.
64. Mollah, M. Y.; Morkovsky, P.; Gomes, J. A.; Kesmez, M.; Parga, J.; Cocke, D. L. Fundamentals, present and future perspectives of electrocoagulation. *Journal of Hazardous Materials* **2004**, *114*, 199-210.
65. Chen, X.; Chen, G.; Yue, P. L. Separation of pollutants from restaurant wastewater by electrocoagulation. *Separation and purification technology* **2000**, *19*, 65-76.
66. El-Naas, M. H.; Alhajja, M. A.; Al-Zuhair, S. Evaluation of a three-step process for the treatment of petroleum refinery wastewater. *Journal of Environmental Chemical Engineering* **2014**, *2*, 56-62.

67. Bhagawan, D.; Poodari, S.; Golla, S.; Himabindu, V.; Vidyavathi, S. Treatment of the petroleum refinery wastewater using combined electrochemical methods. *Desalination and Water Treatment* **2016**, *57*, 3387-3394.
68. Eyvaz, M.; Gürbulak, E.; Kara, S.; Yüksel, E. Preventing of cathode passivation/deposition in electrochemical treatment methods—a case study on winery wastewater with electrocoagulation. In *Modern Electrochemical Methods in Nano, Surface and Corrosion Science*; Aliofkhazraei, M., Ed.; Intech: 2014; pp 201-238.
69. Khandegar, V.; Saroha, A. K. Electrocoagulation for the treatment of textile industry effluent—A review. *Journal of Environmental Management* **2013**, *128*, 949-963.
70. Al Aji, B.; Yavuz, Y.; Koparal, A. S. Electrocoagulation of heavy metals containing model wastewater using monopolar iron electrodes. *Separation and Purification Technology* **2012**, *86*, 248-254.
71. Golder, A.; Samanta, A.; Ray, S. Removal of phosphate from aqueous solutions using calcined metal hydroxides sludge waste generated from electrocoagulation. *Separation and purification technology* **2006**, *52*, 102-109.
72. Kushwaha, J. P.; Srivastava, V. C.; Mall, I. D. Organics removal from dairy wastewater by electrochemical treatment and residue disposal. *Separation and Purification Technology* **2010**, *76*, 198-205.
73. Heikal, M. Effect of temperature on the physico-mechanical and mineralogical properties of Homra pozzolanic cement pastes. *Cement and Concrete Research* **2000**, *30*, 1835-1839.
74. Ge, Q.; Ling, M.; Chung, T. Draw solutions for forward osmosis processes: developments, challenges, and prospects for the future. *Journal of Membrane Science* **2013**, *442*, 225-237.
75. Ng, H. Y.; Tang, W.; Wong, W. S. Performance of forward (direct) osmosis process: membrane structure and transport phenomenon. *Environmental Science & Technology* **2006**, *40*, 2408-2413.
76. Lee, S.; Boo, C.; Elimelech, M.; Hong, S. Comparison of fouling behavior in forward osmosis (FO) and reverse osmosis (RO). *Journal of Membrane Science* **2010**, *365*, 34-39.
77. Mi, B.; Elimelech, M. Organic fouling of forward osmosis membranes: fouling reversibility and cleaning without chemical reagents. *Journal of Membrane Science* **2010**, *348*, 337-345.
78. Mc Ginnis, R. United States Patent US 7560029 B2, 2009.

79. Martinetti, C. R.; Childress, A. E.; Cath, T. Y. High recovery of concentrated RO brines using forward osmosis and membrane distillation. *Journal of Membrane Science* **2009**, *331*, 31-39.
80. Coday, B. D.; Miller-Robbie, L.; Beaudry, E. G.; Munakata-Marr, J.; Cath, T. Y. Life cycle and economic assessments of engineered osmosis and osmotic dilution for desalination of Haynesville shale pit water. *Desalination* **2015**, *369*, 188-200.
81. Phuntsho, S.; Shon, H. K.; Majeed, T.; El Saliby, I.; Vigneswaran, S.; Kandasamy, J.; Hong, S.; Lee, S. Blended fertilizers as draw solutions for fertilizer-drawn forward osmosis desalination. *Environmental Science & Technology* **2012**, *46*, 4567-4575.
82. Wang, J.; Pathak, N.; Chekli, L.; Phuntsho, S.; Kim, Y.; Li, D.; Shon, H. K. Performance of a Novel Fertilizer-Drawn Forward Osmosis Aerobic Membrane Bioreactor (FDFO-MBR): Mitigating Salinity Build-Up by Integrating Microfiltration. *Water* **2017**, *9*, 21.
83. Cath, T. Y.; Drewes, J. E.; Lundin, C. D. A novel hybrid forward osmosis process for drinking water augmentation using impaired water and saline water sources. *Water Research Foundation* **2009**.
84. Achilli, A.; Cath, T. Y.; Childress, A. E. Selection of inorganic-based draw solutions for forward osmosis applications. *Journal of Membrane Science* **2010**, *364*, 233-241.
85. Zhao, S.; Zou, L. Relating solution physicochemical properties to internal concentration polarization in forward osmosis. *Journal of Membrane Science* **2011**, *379*, 459-467.
86. McCutcheon, J. R.; Elimelech, M. Influence of concentrative and dilutive internal concentration polarization on flux behavior in forward osmosis. *Journal of Membrane Science* **2006**, *284*, 237-247.
87. Ling, M. M.; Wang, K. Y.; Chung, T. Highly water-soluble magnetic nanoparticles as novel draw solutes in forward osmosis for water reuse. *Industrial & Engineering Chemistry Research* **2010**, *49*, 5869-5876.
88. Cath, T. Y.; Childress, A. E.; Elimelech, M. Forward osmosis: principles, applications, and recent developments. *Journal of Membrane Science* **2006**, *281*, 70-87.
89. Sitterley, K. A. Evaluating Chemical and Electrocoagulation for the Treatment of Hydraulic Fracturing Wastewater, University of Colorado at Boulder, 2015.
90. Gousmi, N.; Sahmi, A.; Li, H.; Poncin, S.; Djebbar, R.; Bensadok, K. Purification and detoxification of petroleum refinery wastewater by electrocoagulation process. *Environmental Technology* **2016**, *37*, 2348-2357.

91. Sovacool, B. K. Cornucopia or curse? Reviewing the costs and benefits of shale gas hydraulic fracturing (fracking). *Renewable and Sustainable Energy Reviews* **2014**, *37*, 249-264.
92. Beckman, A.; Ambulkar, A.; Umble, A.; Rosso, D.; Husband, J.; Cleary, J.; Sandino, J.; Goldblatt, M.; Horres, R.; Neufeld, R. Considerations for Accepting Fracking Wastewater at Water Resource Recovery Facilities. *Water Environment Federation* **2014**, *20*, 2014.
93. Vigneswaran, S.; Visvanathan, C.; Sundaravadivel, M. Treatment Options for Removal of Specific Impurities from Water. *Wastewater Recycling, Reuse, and Reclamation-Volume II* **2009**, 97.
94. Bazrafshan, E.; Alipour, M. R.; Mahvi, A. H. Textile wastewater treatment by application of combined chemical coagulation, electrocoagulation, and adsorption processes. *Desalination and Water Treatment* **2016**, *57*, 9203-9215.
95. Oncel, M.; Muhcu, A.; Demirbas, E.; Kobya, M. A comparative study of chemical precipitation and electrocoagulation for treatment of coal acid drainage wastewater. *Journal of Environmental Chemical Engineering* **2013**, *1*, 989-995.
96. Xia, J.; Peng, W.; Xiong, R.; Cai, W.; Wei, C.; Zhong, Y. United States Patent US 20110024359 A1, 2009.
97. Sarpola, A. The Hydrolysis of Aluminium: A Mass Spectrometric Study, University of Oulu Oulu, Finland, 2007.
98. Cañizares, P.; Martínez, F.; Jiménez, C.; Lobato, J.; Rodrigo, M. A. Comparison of the aluminum speciation in chemical and electrochemical dosing processes. *Industrial & Engineering Chemistry Research* **2006**, *45*, 8749-8756.
99. Malakootian, M.; Yousefi, N. The efficiency of electrocoagulation process using aluminum electrodes in removal of hardness from water. *Iranian Journal of Environmental Health Science & Engineering* **2009**, *6*, 131-136.
100. Elnenay, A. M. H.; Nassef, E.; Malash, G. F.; Magid, M. H. A. Treatment of drilling fluids wastewater by electrocoagulation. *Egyptian Journal of Petroleum* **2017**, *26*, 203-208.
101. Nan, J.; Yao, M.; Chen, T.; Li, S.; Wang, Z.; Feng, G. Breakage and regrowth of flocs formed by sweep coagulation using additional coagulant of poly aluminium chloride and non-ionic polyacrylamide. *Environmental Science and Pollution Research* **2016**, *23*, 16336-16348.

102. Wiśniewska, M.; Urban, T.; Grządka, E.; Zarko, V. I.; Gun'ko, V. M. Comparison of adsorption affinity of polyacrylic acid for surfaces of mixed silica–alumina. *Colloid and Polymer Science* **2014**, *292*, 699-705.
103. Wiśniewska, M.; Terpiłowski, K.; Chibowski, S.; Urban, T.; Zarko, V.; Gun'ko, V. Effect of polyacrylic acid (PAA) adsorption on stability of mixed alumina-silica oxide suspension. *Powder Technology* **2013**, *233*, 190-200.
104. Das, K. K.; Somasundaran, P. Ultra-low dosage flocculation of alumina using polyacrylic acid. *Colloids and Surfaces A: Physicochemical and Engineering Aspects* **2001**, *182*, 25-33.
105. Sposito, G. *The environmental chemistry of aluminum*; CRC Press: 1995; .
106. Liu, L.; Luo, S.; Wang, B.; Guo, Z. Investigation of small molecular weight poly(acrylic acid) adsorption on  $\gamma$ -alumina. *Applied Surface Science* **2015**, *345*, 116-121.
107. Blandin, G.; Vervoort, H.; D'Haese, A.; Schoutteten, K.; Bussche, J. V.; Vanhaecke, L.; Myat, D. T.; Le-Clech, P.; Verliefde, A. R. Impact of hydraulic pressure on membrane deformation and trace organic contaminants rejection in pressure assisted osmosis (PAO). *Process Safety and Environmental Protection* **2016**, *102*, 316-327.
108. Lee, S.; Kim, J.; Lee, C. Analysis of CaSO<sub>4</sub> scale formation mechanism in various nanofiltration modules. *Journal of Membrane Science* **1999**, *163*, 63-74.
109. Mi, B.; Elimelech, M. Gypsum scaling and cleaning in forward osmosis: measurements and mechanisms. *Environmental Science & Technology* **2010**, *44*, 2022-2028.
110. Dydo, P.; Turek, M.; Ciba, J.; Wandachowicz, K.; Misztal, J. The nucleation kinetic aspects of gypsum nanofiltration membrane scaling. *Desalination* **2004**, *164*, 41-52.
111. Shirazi, S.; Lin, C.; Doshi, S.; Agarwal, S.; Rao, P. Comparison of fouling mechanism by CaSO<sub>4</sub> and CaHPO<sub>4</sub> on nanofiltration membranes. *Separation Science and Technology* **2006**, *41*, 2861-2882.
112. Rahardianto, A.; McCool, B. C.; Cohen, Y. Reverse osmosis desalting of inland brackish water of high gypsum scaling propensity: kinetics and mitigation of membrane mineral scaling. *Environmental Science & Technology* **2008**, *42*, 4292-4297.
113. Colburn, A. S.; Meeks, N.; Weinman, S. T.; Bhattacharyya, D. High Total Dissolved Solids Water Treatment by Charged Nanofiltration Membranes Relating to Power Plant Applications. *Industrial & Engineering Chemistry Research* **2016**, *55*, 4089-4097.

114. Krieg, H. M.; Modise, S. J.; Keizer, K.; Neomagus, H. W. J. P. Salt rejection in nanofiltration for single and binary salt mixtures in view of sulphate removal. *Desalination* **2005**, *171*, 205-215.
115. Le Gouellec, Y. A.; Elimelech, M. Calcium sulfate (gypsum) scaling in nanofiltration of agricultural drainage water. *Journal of Membrane Science* **2002**, *205*, 279-291.
116. Sarti, A.; Zaiat, M. Anaerobic treatment of sulfate-rich wastewater in an anaerobic sequential batch reactor (AnSBR) using butanol as the carbon source. *Journal of Environmental Management* **2011**, *92*, 1537-1541.
117. US EPA Summary of the Technical Workshop on Wastewater Treatment and Related Modeling. **2013**.
118. Chekli, L.; Phuntsho, S.; Kim, J. E.; Kim, J.; Choi, J. Y.; Choi, J.; Kim, S.; Kim, J. H.; Hong, S.; Sohn, J. A comprehensive review of hybrid forward osmosis systems: Performance, applications and future prospects. *Journal of Membrane Science* **2016**, *497*, 430-449.
119. Li, X.; Zhao, B.; Wang, Z.; Xie, M.; Song, J.; Nghiem, L. D.; He, T.; Yang, C.; Li, C.; Chen, G. Water reclamation from shale gas drilling flow-back fluid using a novel forward osmosis–vacuum membrane distillation hybrid system. *Water Science and Technology* **2014**, *69*, 1036-1044.
120. Martinetti, C. R.; Childress, A. E.; Cath, T. Y. High recovery of concentrated RO brines using forward osmosis and membrane distillation. *Journal of Membrane Science* **2009**, *331*, 31-39.

